University of Pretoria

THE EFFECT OF THE Si-Bi_2O_3 SYSTEM ON THE IGNITION OF THE Al-CuO THERMITE

By

KOLELA ILUNGA

A project report submitted in partial fulfilment of the requirements for the degree of

MASTER OF SCIENCE

In the

DEPARTMENT OF CHEMICAL ENGINEERING
FACULTY OF ENGINEERING, BUILT ENVIRONMENT AND INFORMATION TECHNOLOGY
UNIVERSITY OF PRETORIA
PRETORIA

JANUARY 2011

THE EFFECT OF Si-Bi_2O_3 SYSTEM ON THE IGNITION OF THE Al-CuO THERMITE

BY

KOLELA ILUNGA

SUPERVISOR: PROF. WALTER W. FOCKE

DEPARTMENT OF CHEMICAL ENGINEERING

DEGREE: MASTER OF SCIENCE

ABSTRACT

The ignition temperature of the aluminium copper oxide (Al-CuO) thermite was measured using differential thermal analysis (DTA) at a scan rate of 50 °C/min in an inert nitrogen atmosphere. Thermite reactions are difficult to start as they require very high temperatures for ignition, e.g. for the Al-CuO thermite comprising micron particles it is ca. 940 °C. It was found that the ignition temperature is significantly reduced when the binary Si-Bi_2O_3 system is used as sensitiser. Further improvement is achieved when nano-sized particles are used. For the composition CuO + Al + Bi_2O_3 + Si (65.5:14.5:16:4 wt %), when all components except the aluminium fuel are nano-sized, the observed ignition temperature is reduced to ca. 615 °C and results in a thermal runaway.

Keywords: Pyrotechnics; Thermite; Ignition temperature; Nanoparticles; Melting temperature; Tender.

ACKNOWLEDGEMENTS

I am grateful to:

Professor Walter Focke for his supervision and pertinent suggestions throughout this dissertation. Thank you very much.

Mr Ollie del Fabbro, Mrs Milla Maksa, Mrs Priscilla Appana and Mrs Pravina Maharaj for their assistance during the course of this research.

AEL Mining Services for their technical and financial support.

My parents – Marcel Ilunga and Petronie Odia – thank you for bringing out the best in me through your advice.

Bibiche Mbombo for your patience, help and understanding during my studies.

Pedro Massinga, Arao Manhique, Nontete Nhlapo, Lumbi Moyo, Darren Swanepoel and Dan Molefe – my colleagues at the Institute of Applied Materials, University of Pretoria. Your support is gratefully acknowledged.

Lord Jesus Christ, you will show me the way of life, granting me the joy of your presence and the pleasures of living with you forever. Blessed be your magnificent name.

DECLARATION

I, the undersigned, declare that the dissertation that I hereby submit for the degree Master of Science at the University of Pretoria is my own research, and has not previously been submitted by me for degree purposes or examination at this or any another university.

Pretoria, January 2011

Kolela Ilunga

TABLE OF CONTENTS

LIST OF FIGURES

LIST OF TABLES

LIST OF ABBREVIATIONS AND SYMBOLS

A	Absorptivity of the composition
AEL	African Explosives Limited
b	Length of the reaction zone
C_p	Specific heat capacity
DC	Direct current
DSC	Differential scanning calorimetry
DTA	Differential thermal analysis
E_a	Activation energy
E_f	Efficiency of thermal energy feedback
F_{fb}	Fraction of energy fed back
H_r	Heat of reaction
K	Rate of a simple pyrotechnic chemical reaction
Mox	Molecular weight of oxygen
Mred	Molecular weight of reducing agent
n	Number of moles
OB	Oxygen balance
P	Specific ignition stimulus applied
Q_G	Rate of heat gain by a pyrotechnic composition
Q_L	Rate of heat loss from the centre of pyrotechnic composition
R	Gas constant
RT	Gas constant
S	Surface illuminated by the laser
SEM	Scanning electron microscope/microscopy
SSA	Specific Surface Area
T_a	Ambient temperature
T_{ad}	Adiabatic flame temperature
t_{ign}	Time to ignition
T_{ign}	Ignition temperature
T_r	Thermal runaway temperature
u	Number of oxygen atoms in the oxidiser

UV	Ultra-violet
V_B	Burning velocity of pyrotechnic
Wt	Weight
XRD	X-ray diffraction

GREEK SYMBOLS

Δ	Variation
ξ	Constant derived from geometry and thermal properties of the pyrotechnic material
ρ	Bulk density
λ	Thermal conductivity

CHAPTER 1 INTRODUCTION

1.1 Problem Statement

Thermites are a subclass of pyrotechnic materials that usually contain aluminium (Al) as the fuel and an oxidiser such as a metal oxide (e.g. copper oxide, CuO). Thermite reactions can be ignited by a combustion wave from a chemical reaction, an electric current, radiation energy from a laser beam or mechanical impact (Munir, 1988). Once initiated, Al fuel is combined with a metal oxidiser and such a reaction may exceed an adiabatic flame temperature of 2 000 K. The ignitability of a thermite is an extremely important performance parameter. Knowledge of the ignition temperature and the time to ignition allow thermite materials to be tailored for specific applications (e.g. military, mining and cutting torches).

The main drawbacks of using thermite reactions utilising micron-sized aluminium powder fuels are long ignition delays, slow burn rates and incomplete combustion (Shoshin and Mudry, 2002). Initiation of a metal-metal oxide redox reaction is quite difficult for mixtures of micron-sized powders and requires extended preheating of a relatively large or a well-heat-insulated sample. Due to the high thermal conductivity of metal–metal oxide mixtures, small, poorly insulated samples lose heat very rapidly, and for such samples the initial heterogeneous reaction never becomes self-sustaining (Edward, 2009). Often the ignition temperature of a thermite composition is extremely high. Furthermore, the required ignition temperatures cannot be reached with conventional ignition sources such as black powder fuses, nitrocellulose rods, detonators, a suitable pyrotechnic initiator or other common igniting substances (Wang *et al.*, 1993). These problems explain the very limited range of applications of conventional thermite compositions.

1.2 Aim of the Research

A major benefit of thermite compositions is their immunity to accidental ignition (German and Ham, 1979). This makes them particularly interesting as a replacement candidate for primary explosives in conventional detonators. The aim of the present research is to explore further sensitisation of the Al-CuO thermite system by the fast-burning Si + Bi_2O_3 pyrotechnic composition used as tinder, for both micron-sized and nano-sized thermite mixtures.

1.3 Historical Background

There are several ways to light a thermite mixture safely, the most common being (Shakhashiri, 1989):

- **A propane torch:** This should never be attempted for safety reasons. The torch can preheat the entire pile of thermite, which can cause it to explode instead of burning when it finally reaches ignition temperature.

- **Strips of magnesium metal used as fuses:** Mg metal is difficult to ignite (2 500 K). A significant danger of this method is the fact that Mg metal is an excellent conductor of heat. So, heating one end of the ribbon may cause the other end to transfer enough heat to cause premature ignition of the thermite.

- **The reaction between $KMnO_4$ and glycerine:** Some glycerine is poured over $KMnO_4$. Eventually a spontaneous reaction will start and slowly increase the temperature of the mixture until flame is produced. The heat released by the oxidation of glycerine is sufficient to initiate a thermite reaction. However, the delay between mixing and ignition can be greatly affected by the ambient temperature.

- **A common sparkler to ignite the mix:** These materials may reach the necessary temperatures but require a sufficient amount of time before the burning point reaches the thermite.

Most of the above methods used to initiate thermite reactions are too unreliable to be incorporated into the design of a pyrotechnic device. This has restricted practical applications of conventional thermite reactions.

Adding small amounts of aluminium fluorite or cryolite ($NaAlF_6$) reduces the ignition temperature and can double the burn rate (Wang *et al.*, 1993). These performance improvements are attributed to the salts removing the inert reaction-inhibiting alumina coatings on aluminium at temperatures significantly lower than the ignition temperature (Wang *et al.*, 1993).

Reducing the particle size of the fuel into the nanometre range is much more effective as the interface area is substantially increased (Aumann *et al.*, 1995; Bockmon *et al.*, 2005; Stamatis *et al.*, 2009). The use of nano-aluminium as fuel enhances ignition sensitivity, i.e. it reduces ignition delay and lowers the ignition temperature (Granier and Pantoya, 2004; Hunt and Pantoya, 2005; Stamatis *et al.*, 2009). Granier and Pantoya (2004) attribute this to the increased surface energy associated with nanoparticles, an effect that also leads to a reduction in the melting point.

1.4 Focus of the Investigation

Thermite reaction utilising a metal oxidiser such as CuO can be very explosive (Prakash, 2004). Although the Al-CuO thermite mixture does not produce the same amount of energy as some other compositions, such as iron (II, III) oxide, the Al-CuO thermite system has an incredibly fast burn rate. In addition, copper has a comparatively low melting point. During the reaction, drops of molten copper are sent out because the mixture has a tendency to explode.

Consequently, nano-thermite mixtures have been found difficult to process safely. The main difficulty is in the handling of dry nano-sized powder mixtures due to their sensitivity to friction and the electrostatic discharge of nano-aluminium fuel (Erickson *et al.*, 2008). Therefore, for safety reasons, the ease of ignition based on the particle size of the fuel is sometimes sacrificed to some extent and larger particle sizes are used to minimise accidental ignition by static discharge (Conkling, 1985).

The present work concentrates on the effect of the Si-Bi_2O_3 pyrotechnic composition on the ignition of the Al-CuO thermite system. Differential thermal analysis (DTA) ignition studies were used to show that the ignition temperature can be reduced significantly when both nano-sized and micron-sized aluminium fuels are used.

It has been reported that the pyrotechnic Si-Bi_2O_3 composition, with a ratio of 20% Si to 80% Bi_2O_3, can be used for a short-time-delay composition with a maximum burn rate of 156 mm/s (Kalombo *et al.*, 2004). This composition is sensitive to heat and its reaction temperature is about 1 100 ℃. Therefore, the Si-Bi_2O_3 pyrotechnic composition can be added as 'tinder' to lower the ignition temperature of both nano-sized and micro-sized Al-CuO thermite systems.

1.5 Outline of the Investigation

Chapter 1 is the introduction, in which the research problem is posed, the aim of the work presented, and the structure of the dissertation outlined.

Chapter 2 reviews the literature on pyrotechnic materials in general.

Chapter 3 outlines the experimental design. The raw materials and the instruments used for the laboratory work are presented. The methods and procedures followed in the laboratory are described.

Chapter 4 analyses and discusses the experimental results.

Chapter 5 presents the conclusions and makes recommendations for possible further study.

In Chapter 6, all the references used are listed.

Additional supporting information is given in the Appendices

CHAPTER 2 COMPOSITE ENERGETIC MATERIALS

2.1 Introduction

Pyrotechnics are a subclass of energetic materials that release their energy in a short time interval during exothermic chemical reactions. They operate, when initiated, by a self-sustaining combustion process in which a fuel combines with the oxygen released by a metal oxidiser to create fire, heat, light, smoke or gas emission but not explosions (Charsley *et al.*, 2001).

Pyrotechnic devices include matches, flares, smoke grenades, airbag inflators, military incendiaries, solid rockets, fuel pellets for field stoves and other heating units, as well as in quick-release devices used for emergency exit systems in aircraft, or for staging and shroud ejection systems in space launch vehicles (Conkling, 1990). Pyrotechnic powders are also pressed into rigid time-delay elements used in non-electronic detonators. Time-delay elements allow the desired interval between an impulse and a later detonation of the main blasting charge. Pyrotechnic compositions are usually compacted to make pellets. Their reactions can be provoked by a specific ignition stimulus such as flame, impact, static spark, high ambient temperatures or a laser beam.

Thermites are a subclass of pyrotechnics in which an oxophilic metal such aluminium (Al), magnesium (Mg), zircon (Zr), titanium (Ti) or boron (B) is oxidised by an oxide of another metal. They are characterised by a very large heat release (Fisher and Grubelish, 1998). The adiabatic reaction temperature exceeds the melting point of at least one of the products (Wang *at al.*, 1993). Usually, thermite reactions are extremely exothermic, with temperatures exceeding 2 000K. Thermites with nano-sized particles are described by a variety of terms, such as metastable intermolecular composites, superthermite (Erickson *et al.*, 2008), nanothermite, and nanocomposite energetic materials (Gash *et al.*, 2002).

Thermite formulations have been created for use in cutting torch and welding applications. The thermite operates by exposing a very small area of metal to extremely high temperatures. Intense heat focused on a small spot can be used to cut through metal or weld metal components together both by melting metal from the components, and by injecting molten metal from the thermite reaction itself (Wang *et al.*, 1993).

Thermite usage is hazardous due to the extremely high temperatures produced and the extreme difficulty in smothering a reaction once initiated. The thermite reaction releases dangerous ultra-violet (UV) light requiring that the reaction not be viewed directly, or that special eye protection (i.e. a welder's mask) be worn. Small streams of molten metal released in the reaction can travel considerable distances and may melt through metal containers, igniting their contents. It is recommended to be very careful when attempting to ignite thermite compositions.

2.2 Pyrotechnic Compositions

The basic components of any pyrotechnic composition are the oxidiser and the reducing agent (fuel). Other optional constituents are binders, propellants, colouring agents, and sound- or smoke-producing agents. Binders are important constituents of pyrotechnics and are usually represent several weight per cent of the pyrotechnic charge. Their main role is preventing the segregation of mixtures into their components during manufacture, transport and storage.

Ordinary oxidisers and fuels used in the manufacturing of composite energetic materials are listed in Table 2.1.

Table 2.1: Composition of ordinary oxidisers and fuels used in pyrotechnics (Rugunanan, 1991)

Oxidants	Fuels (non metals)	Fuels (metals)
Chlorates	Boron	Aluminium
Chromates	Carbon	Chromium
Dichromates	Dextrose	Iron
Iodates	Lactose	Magnesium
Nitrates	Naphthalene	Manganese
Oxides	Phosphorus	Molybdenum
Perchlorates	Selenium	Titanium
Peroxides	Silicon	Tungsten
Permanganates	Sulphur	Zirconium
Sulphates	Sucrose	

2.3 Oxygen Balance

Pyrotechnic compositions undergo a self-sustaining exothermic solid-solid state reduction/oxidation reaction that provides its own oxygen supply and does not require any external source such as atmospheric oxygen for combustion (Wilson and Hancox, 2001).

The potential of an oxidiser in a pyrotechnic reaction is determined primarily by the oxygen balance. This value (in percentage) represents the theoretical ability of a pyrotechnic system to perform complete combustion (Steinhauser and Klapotke, 2008).

The oxygen balance of a pyrotechnic redox system is given by the following equation (1) (Berger, 2005):

$$OB(\%) = 100 \frac{nox\ Mox\ u}{nred Mred + nox Mox} \tag{1}$$

Where

Mox is the molecular weight of oxygen
Mred is the molecular weight of reducing agent
u is the number of oxygen atoms in the oxidiser
n is the number of moles

A composition of a pyrotechnic system with an equalised oxygen balance (50:50) generally shows the highest energy released, but not the highest reaction rate. This is due to the fact that pyrotechnic reactions are usually solid-solid state reactions (Berger, 2005).

2.4 Solid-solid State Reaction of Pyrotechnic Materials

2.4.1 Solid state

Pyrotechnists care about chemical bonds because of that the way pyrotechnic energy is produced. Most solid oxidisers that are formed naturally in the earth have a homogenous structure in which their atoms are arranged in a regular repeated pattern (Figure 2.1). The solids are crystalline and their repeated units are linked together in different ways: covalent (electron sharing), ionic (electron transfer), metallic, or sometimes hydrogen and Van der Waals bonds.

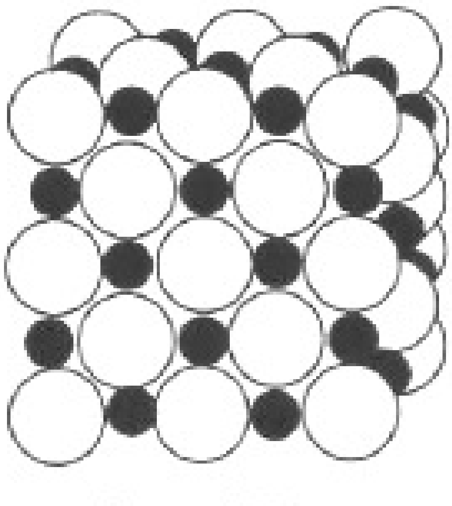

Figure 2.1: Three-dimensional pattern for crystalline solids

Crystalline solids are not single and perfect crystals; they are composed of small crystals joined at boundaries that form discontinuities in the structure called ‘points defects’ (McLain, 1979). Local disturbances causing points defects can be: a vacancy, a substitution impurity or interstices.

When a neighbouring site is vacant, however, an atom can easily jump into this site, thus changing places with the vacancy. The vacancy moves in the opposite direction to the site, which used to be occupied by the moving atom. Therefore slow diffusion occurs in crystalline solid materials (Guy, 1976).

2.4.2 Reactivity

Pyrotechnic reactions are one type of solid-solid state oxidation-reduction reaction. As temperature rises, vibrational energy increases. At some point the vibrational motions become so great that the rigid structure of solids oxidisers breaks down (Kosanke *et al.*, 2004; Van Vlack, 1970). An oxidation-reduction reaction necessitates the transfer of electrons from the fuel (reductor) to the oxidising agent (electron acceptor). Pyrotechnic combustion differs from normal combustion in that the source of oxygen is not from the air, but rather it is from oxygen-rich oxidisers. Solid-solid state reactions consist of initial formation of solid product(s) that spatially separate the reactants. Reactants migrate through the conductive product layer only as ions and electrons also have to accompany the ions' movements (McClain, 1979).

Subsequent reaction requires:

- that reactants and product layers must be able to conduct electrons
- the presence of lattice defects in the structure of the composite energetic material
- intimate contact between the components which reduces diffusion distances between oxidiser and fuel components
- homogeneity of the powder (good mixing): domains rich in either fuel or oxidiser limit mass transport and therefore decrease the efficiency of the reaction.

Pyrotechnic compositions that contain metallic fuel, great disorder, channels, components with a high specific surface area and other effects of microstructure (crystal form) are generally reactive. Furthermore, solid-solid state reaction kinetics is controlled largely by mass transport rates between reactants (Tillotson *et al.*, 2001).

2.5 Energy Considerations for Pyrotechnic Reactions

A pyrotechnic reaction can be considered as taking place in two steps. First, energy ('activation energy') must be input to the system. Second, energy ('heat of reaction') is produced by the reaction (Figure 2.2).

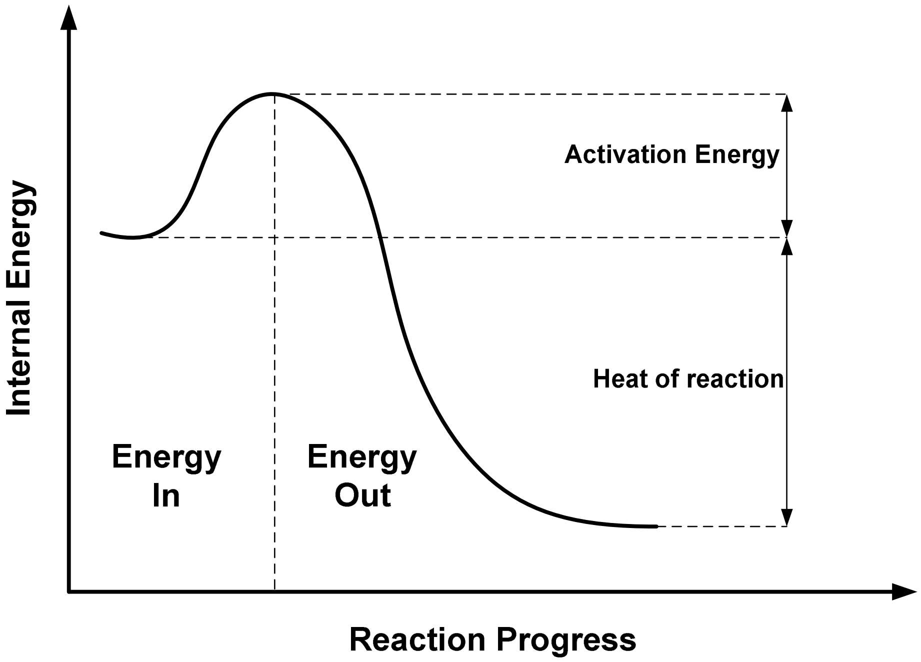

Figure 2.2: Effect of internal energy on reaction progress

The first step can be thought of as the breaking of the original chemical bonds, and the second step as the forming of new and stronger chemical bonds (Kosanke *et al.*, 2004).

2.5.1 Thermal energy distribution of atoms in fuel and oxidiser particles in pyrotechnic compositions

Figure 2.3 illustrates the distribution of the thermal energy of individual atoms in fuel and oxidiser particles in a pyrotechnic composition at a particular temperature, T_1. The curve goes through the origin of the graph, meaning that zero atoms have zero energy. Thereafter an increasing number of atoms have increasing energy, until a peak is reached, followed by a continuously decreasing number of atoms possessing higher energies (Kosanke *et al.*, 2004). In this figure, the activation energy E_a is known as the energy required to initiate the pyrotechnic reaction.

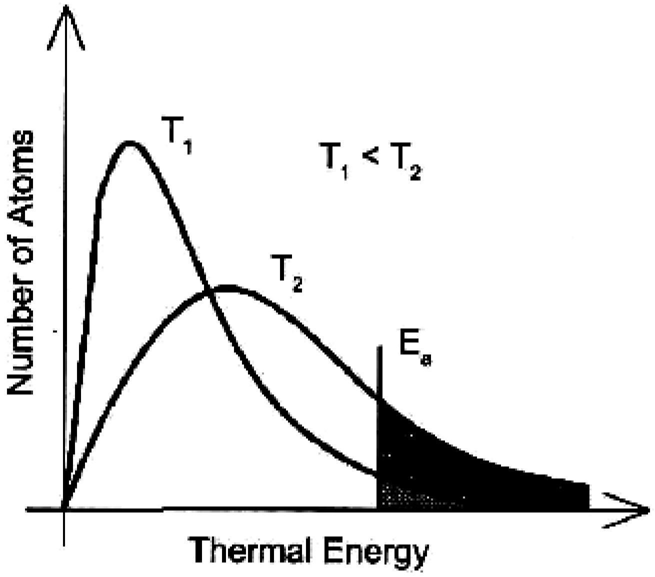

Figure 2.3: Distribution of the thermal energy of individual atoms in fuel and oxidiser

If the temperature of the pyrotechnic composition is raised, from T_1 to a higher temperature T_2, on average the atoms jostle around with more energy. More significantly, the number of atoms with energies exceeding the activation energy barrier increases greatly. As a consequence, there are now many more atoms capable of reacting and there is a corresponding increase in the rate at which the reactions occur. These chemical reactions produce thermal energy; thus an increase in the reaction rate causes an increase in the rate of production of heat. This produces a further increase in temperature, which causes still more atoms to have energies exceeding the activation energy barrier, which in turn causes a still greater increase in the reaction rate and the rate of heat production. This accelerating cyclic process is outlined in Figure 2.4 and leads to what can be called ‘thermal runaway’ and ignition (Kosanke *et al.*, 2004).

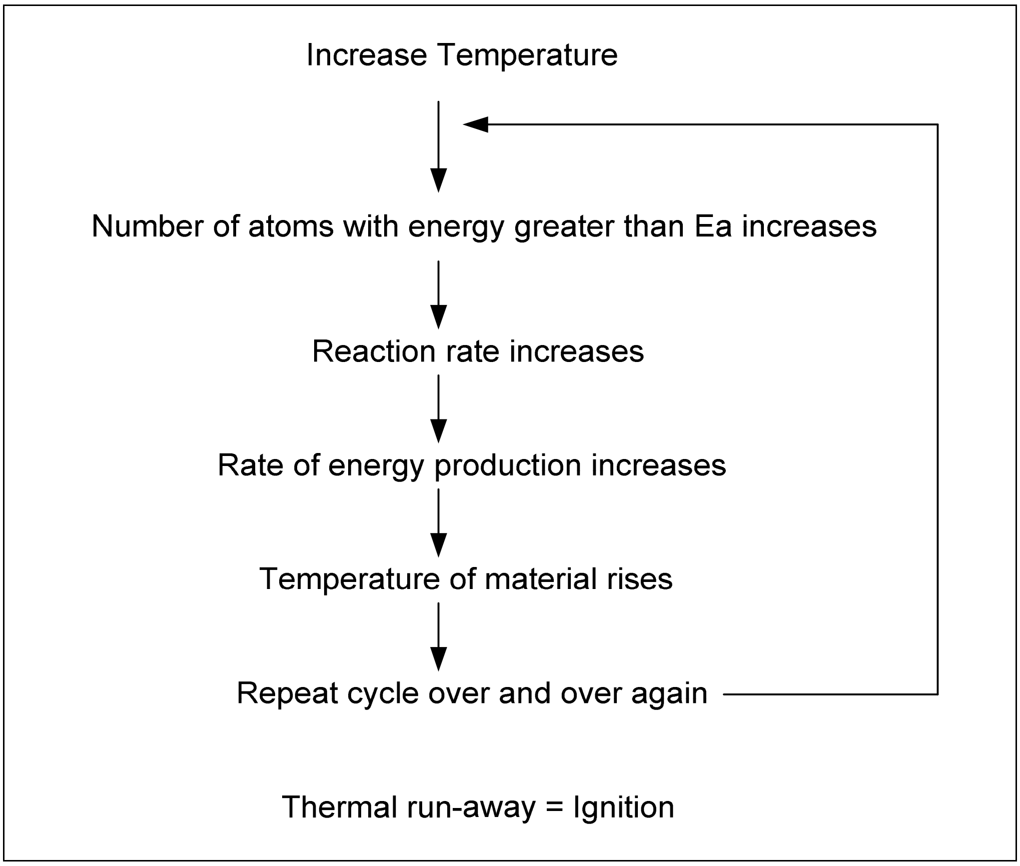

Figure 2.4: Effect of increasing temperature of pyrotechnic compositions

2.5.2 Rates of heat loss and heat gain of pyrotechnic compositions

For a mass of pyrotechnic composition, heat loss from the surface will be primarily from convection through contact with the air. However, any heat generated internally will first need to be conducted to the surface. The rate of heat loss Q_L from the centre of the pyrotechnic composition depends on the thermal conductivity of the composition and any packaging, the convective heat loss coefficient, the geometry of the sample, and the difference in temperature between the centre of the composition T and the ambient temperature T_a. This may be expressed approximately by equation (2) (Weston and Zemansky, 1970), with ξ being a constant derived from the geometry and thermal properties of the pyrotechnic sample. Therefore, the rate of heat loss increases linearly and the line crosses the temperature axis at ambient temperature with a slope equal to ξ.

$$Q_L = \xi (T - T_a) \tag{2}$$

The rate k of a simple pyrotechnic chemical reaction follows an exponential relationship, sometimes referred to as the Arrhenius equation. The rate of heat gain Q_G is the reaction rate multiplied by the heat of reaction as expressed by equation (3) (Mahan, 1965).

$$Q_G = k.\ \Delta H_r \tag{3}$$

Thus, the curve of the rate of heat gain passes through the origin and rises exponentially with increasing temperature.

2.5.3 Effect of increasing temperature on rates of heat loss and heat gain

The effect of increasing temperature on the rates of heat loss and gain is illustrated in Figure 2.5 (Kosanke *et al.*, 2004). At ambient temperature, the rate of heat loss is zero, while the rate of heat gain is greater than zero. Accordingly, the temperature of the sample will begin to increase. The temperature of the sample will continue to rise until the rate of heat gain and loss are equal. This occurs at the crossing point of the ‘gain’ and ‘loss’ curves, where the temperature of the sample T_S has risen to slightly above T_a. When the pyrotechnic composition is momentarily raised from T_S to T_1 somewhat more above T_a, the rate of energy production and the rate of energy loss both increase. However, the rate of loss increases more than the rate of gain (production).

Accordingly, the net effect will be a loss of thermal energy with time. Then the temperature of the pyrotechnic composition will decrease and must continue to fall to the temperature where the rates of loss and gain are equal at T_S. This explains why pyrotechnic compositions are at least meta-stable, in that any small addition of energy will not ultimately cause thermal runaway and ignition.

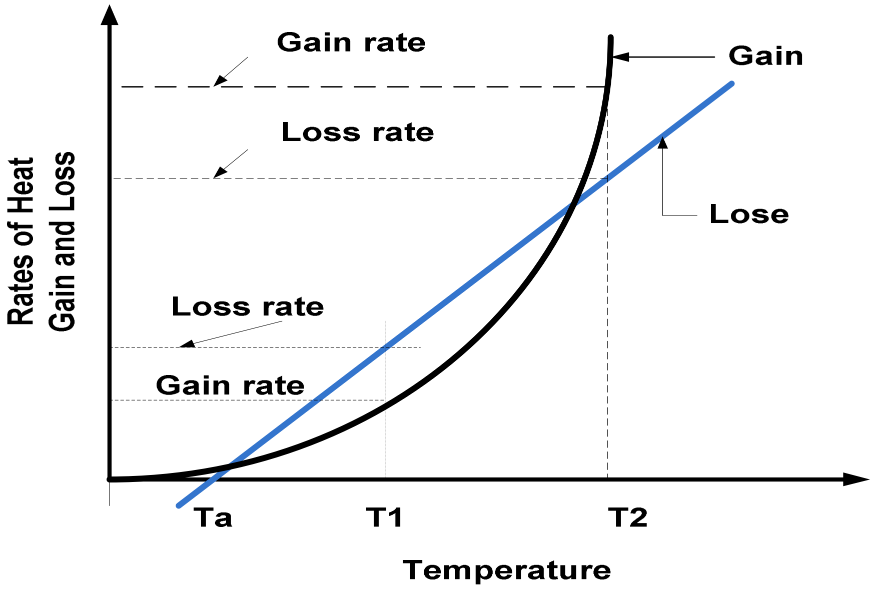

Figure 2.5: **Effect of increasing temperature on rates of heat loss and gain**

If the temperature is raised to T_2, above the second crossing point of the curves, the result are quite different. In this case, again both the rate of heat loss and heat gain increase. However, this time the rate of heat gain has overtaken the rate of heat loss. Therefore, at this temperature, there is a net accumulation of the producing heat and a further increase in temperature. In fact, this is an ever-accelerating process because as the temperature increases, the rate of gain increases much faster than the rate of loss. Then the process leads to thermal runaway and ignition.

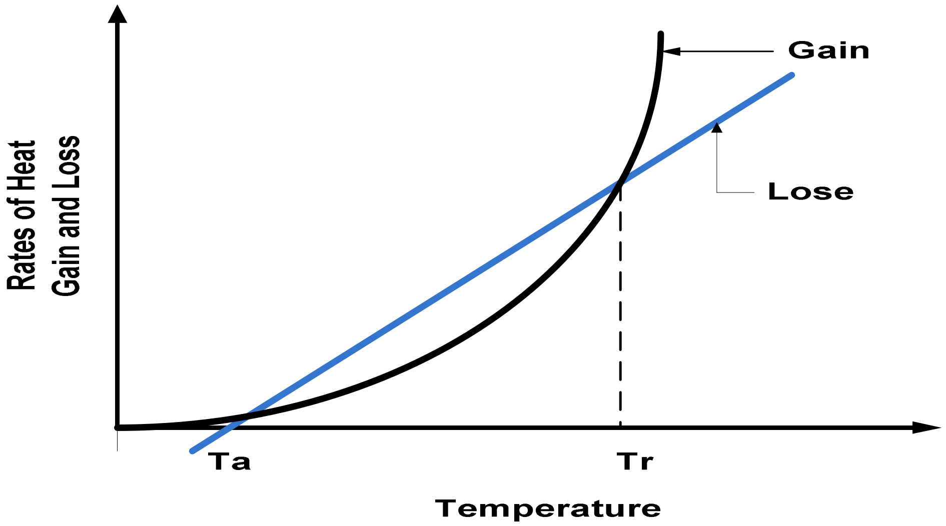

Figure 2.6: **Thermal runaway temperature under known conditions**

In Figure 2.6, the temperature corresponding to the point where the gain and loss curves cross on the graph for the second time can be called the ‘thermal runaway temperature’ T_r.

2.5.4 Effect of increasing sample size on the rate of heat loss

The rate of heat gain (per g of composition) is unaffected by sample size, but the rate loss is dependent on sample size. Generally, as shown in Figure 2.7, small samples lose heat easily and have a rate of heat-loss curve that is steep, with two crossing points, the higher of which is the thermal runaway temperature (Kosanke *et al.*, 2004).

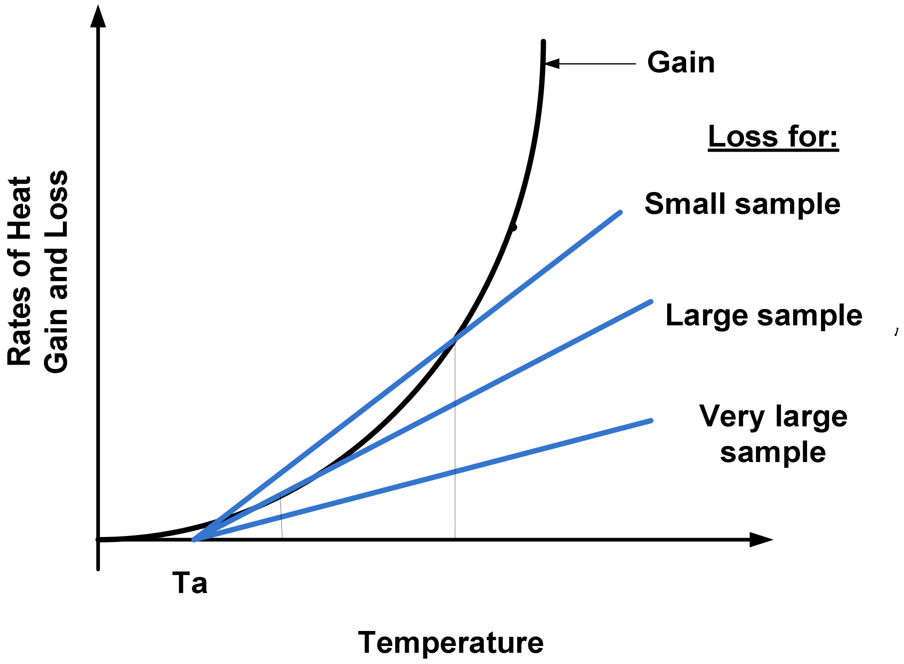

Figure 2.7: Effect of sample size on the rate of heat loss

As the sample size increases (medium sample size), the slope of the heat-loss curve decreases, lowering the runaway temperature more and more with increasing sample size. At some point, for a large sample, there will only be a single point of contact between the curves. This represents the largest sample, under a specific set of conditions, that theoretically will not spontaneously run away thermally and ignite. For samples larger than this, the rate of heat gain is always more than the rate of loss, and the sample will always run away thermally.

It may take a very long time, but for samples that are large enough, eventually there must always be a spontaneous ignition.

2.5.5 Effect of increasing ambient temperature on the rate of heat loss

The effect of ambient temperature on the rate of heat loss is illustrated in Figure 2.8 (Kosanke *et al*., 2004). When the ambient temperature is low (T_{a1}), the sample loses heat to the surroundings quite easily. This places the heat-loss rate curve quite high on the heat-gain curve, producing two crossing points, the higher of which is the thermal runaway temperature. As the ambient temperature increases, it becomes more difficult for the sample to lose heat. The slope of the heat-loss curves is unchanged, but their positions relative to the heat-gain curves are lower. Thus the runaway temperature is lowered more and more with increasing ambient temperatures.

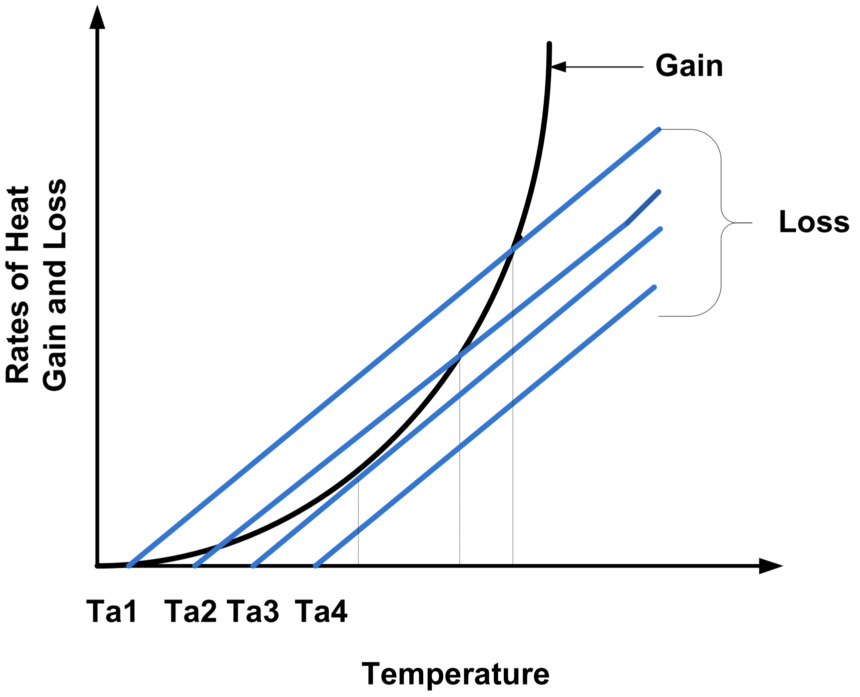

Figure 2.8: Effect of increasing ambient temperature on heat loss

At some point, for a sufficiently high ambient temperature (T_{a3}), there will be only a single point of contact between the curves. This represents the highest ambient temperature, for this type and size of sample, that will not spontaneously run away thermally. For an ambient temperature greater than this, the rate of heat gain is always more than the rate of heat loss, and the sample will always run away thermally. It may take a long time, but for such hot ambient conditions there will eventually be a spontaneous ignition.

Just how large a sample and just how high an ambient temperature are required for thermal runaway and spontaneous ignition depends on the chemical formulation and the conditions of its packaging and storage.

2.5.6 Ignition temperature

The ignition temperature of pyrotechnic compositions (T_{ign}) is of considerable importance both from the point of view of designing pyrotechnic devices and from the safety aspect. The ignition temperature can be defined as the minimum temperature to which an energetic material must be heated in order to provoke a self-sustaining reaction. The reaction zone emits enough heat to bring the adjacent layer to the same temperature as that of the reactants without additional heating by an external source (McLain, 1979).

The ease of ignition also depends on the particle size of the components in the pyrotechnic mixture. However, fine metallic powders can be very hazardous substances since they react readily in air (pyrophoric). For instance, aluminium or magnesium may be hazardous when present in fine particle sizes (< 5 microns). Thus for safety reasons, ease of ignition based on the particle size of fuels is sacrificed to some extent and larger particle sizes are used to minimise accidental ignition by static discharge (Conkling, 1985).

For a pyrotechnic reaction to occur, the atoms (or molecules) must have the required activation energy, and they must be in direct contact with other atoms of the correct type. Even for well-mixed solid particles, there are relatively few points of contact between individual particles (Figure 2.9). Thus, the number of fuel and oxidiser atoms that are in contact with one another is normally quite small.

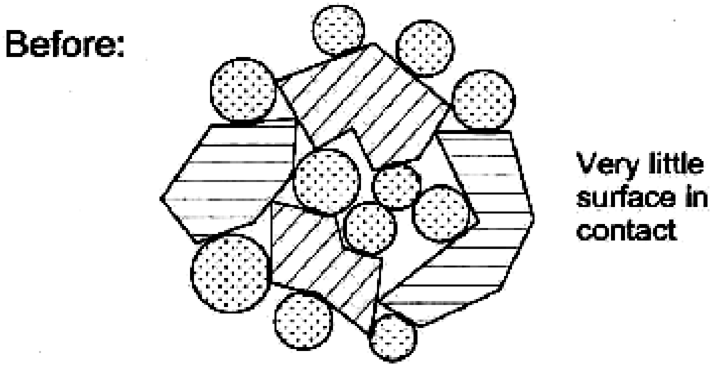

Figure 2.9: Physical contact of solid particles before melting

After one component melts, it is free to flow over the surface of the other components. The number of fuel and oxidiser atoms in physical contact is then very much greater (Figure 2.10). More atoms with energy exceeding E_a are now in contact and will react. The rate of reaction increases and the rate of energy production increases too. Thermal runaway then occurs at a lower temperature.

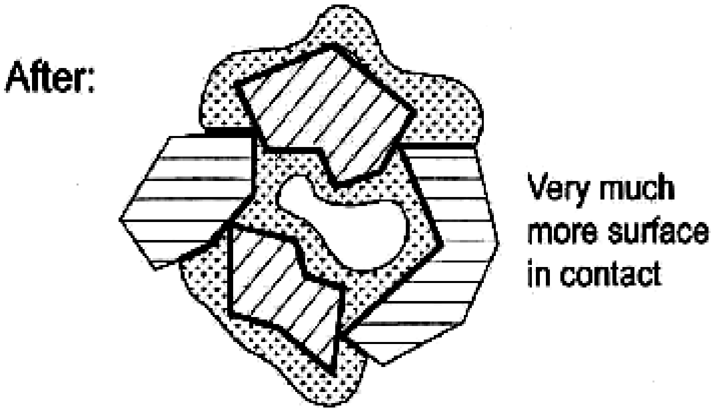

Figure 2.10: Physical contact of solid particles after melting of one component

Thus, as a pyrotechnic composition is heated and nears its ignition temperature, if one of its components reaches its melting point, ignition will generally occur at that temperature (Kosanke *et al.*, 2004).

The ignition temperature of a pyrotechnic composition can also be influenced by pyrotechnic catalysts (Kosanke *et al.*, 2004), which are a special class of pyrotechnic additives. Catalysts are chemicals (generally not consumed in the reaction) that increase the rate of the reaction. However, pyrotechnic catalysts are often consumed because of high temperatures during burning.

Burn catalysts often act by lowering the activation energy or by lowering the decomposition temperature of an oxidiser. The reduction of the oxidiser's decomposition temperature acts to lower the ignition temperature and reduces the time required to reach the now lower ignition temperature (Kosanke *et al.*, 2004).

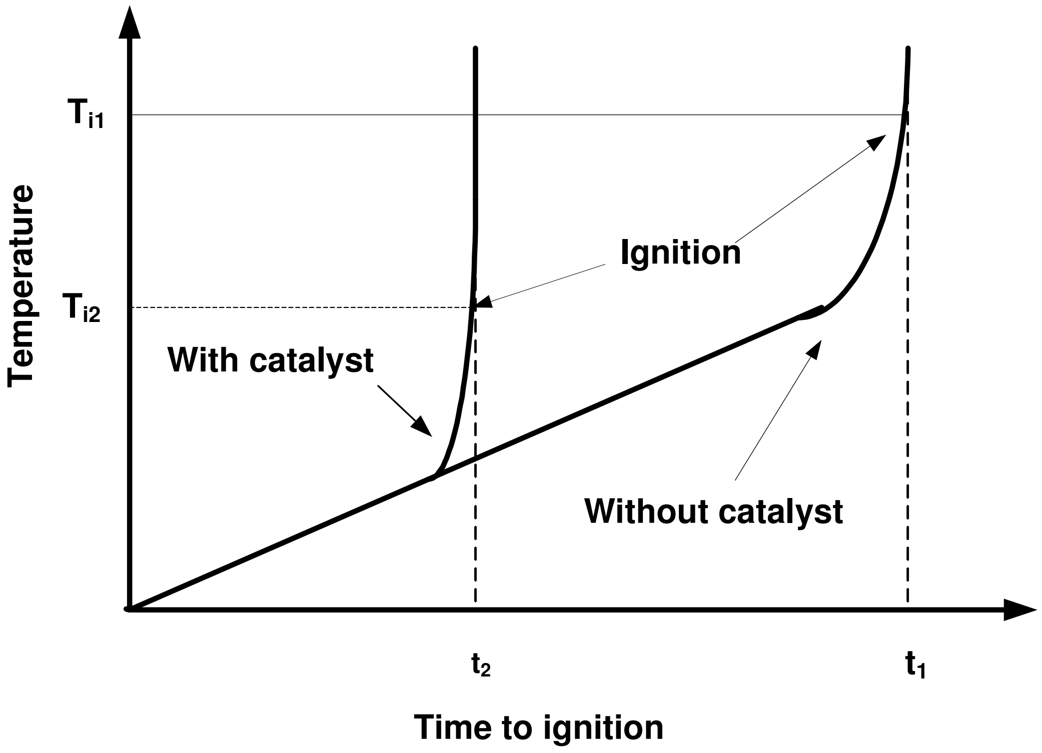

Figure 2.11: Effect of a catalyst on the ignition of pyrotechnics

Figure 2.11 illustrates that if the addition of a burn catalyst lowers the ignition temperature (i.e. from T_{i1} to T_{i2}), less time will be required for each layer of the pyrotechnic composition to be heated to its ignition temperature (i.e. $t_2 < t_1$).

2.5.7 Time to ignition

The time before ignition is an important factor that determines the sensitivity of an energetic material to a specific ignition stimulus. The time for any pyrotechnic composition to ignite is a function of the temperature to which it is exposed, as illustrated in Figure 2.12 (Kosanke *et al.*, 2004).

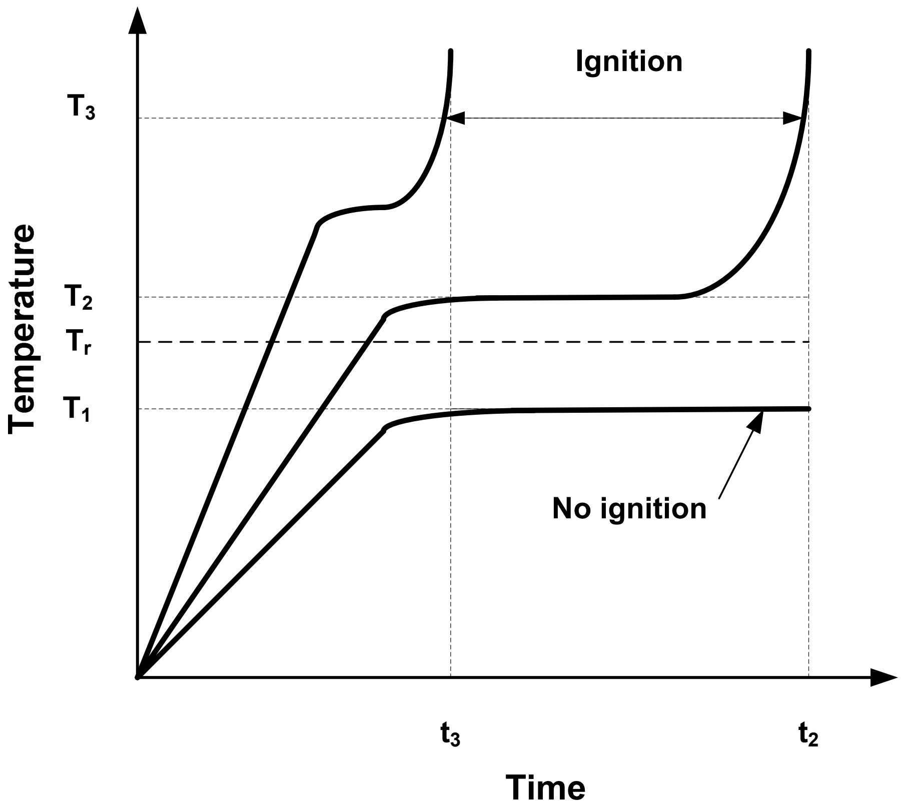

Figure 2.12: Time to ignition of pyrotechnic materials for initially cold samples placed in an oven at constant temperature

When a sample is placed in an oven, its temperature will begin to rise, eventually reaching the temperature of the oven. If the temperature of the oven T_1 is less than T_r for pyrotechnic runaway, the sample will never ignite (i.e. time to ignition is infinite).

When the temperature of the oven is increased to T_2, slightly above T_r, the sample will start to heat up and will eventually rise to the temperature of the oven. For a while, it may appear that nothing is happening with the sample. However, inside the sample, heat is slowly accumulating, raising the temperature. As the internal temperature rises, the rate of reaction increases, increasing the rate of heat gain, and further increasing the temperature (i.e. runaway temperature has begun). As a result of this even accelerating process, the internal temperature rises even more rapidly, until eventually there is an ignition at time t_2.

If the temperature of the oven temperature is increased to T_3, significantly higher than T_r, the sample will heat up, approaching the oven temperature. However, under these conditions, the sample's temperature rise is very much faster as it reaches the oven temperature. The time to ignition t_3 becomes increasingly short, until it appears to be nearly instantaneous.

Equation (4) below is used to estimate ignition delay times caused by laser heating ignition (Schoenitz and Dreizin, 2005).

$$t_{ign} = \frac{\pi\lambda\rho C(Ti-To)^2}{4(\frac{AP}{S})^2} \tag{4}$$

This equation explains a number of physical facts that generally conform to expectations based on both experience and intuition. The time to ignition is longer (Schoenitz and Dreizin, 2005) if:

- The heat dissipates rapidly (high thermal conductivity λ)
- There is a higher ratio of mass to heat (high density ρ)
- More heat is required per unit mass (C) to raise the temperature
- A significant surface area (S) is illuminated by the laser, resulting in heat loss (large cross-sectional area)
- A higher ignition temperature (T_i) is required.

The ignition time is shorter if the absorptivity (A) of the composition or the specific ignition stimulus applied (P) is high because more heat is available to raise the temperature (Schoenitz and Dreizin, 2005).

2.6 Sensitivity

A pyrotechnic material with a given powder confinement is said to be ‘sensitive’ to certain ignition stimuli (i.e. impact, heat, friction, static spark or laser beam) if it ignites and self-propagates easily when that specific ignition stimulus is applied (McLain, 1979). Sensitivity is a measure of the stimulus required to cause reliable design-mode functioning of an energetic material (Kosanke *et al.,* 2004).

Because the incendiary and explosive output of pyrotechnic materials can be equally devastating, rating their hazard can amount to rating their potential for accidental ignitions, known as FISH (Friction, Impact, Static discharge and Heat).

2.6.1 Friction sensitivity

Friction sensitivity is a measure of a material's tendency to ignite in response to energy input as friction. Often a sample is placed between two ceramic surfaces (one rounded and one flat), which are pressed together. In the test, the two surfaces are moved relative to each other as shown in Figure 2.13.

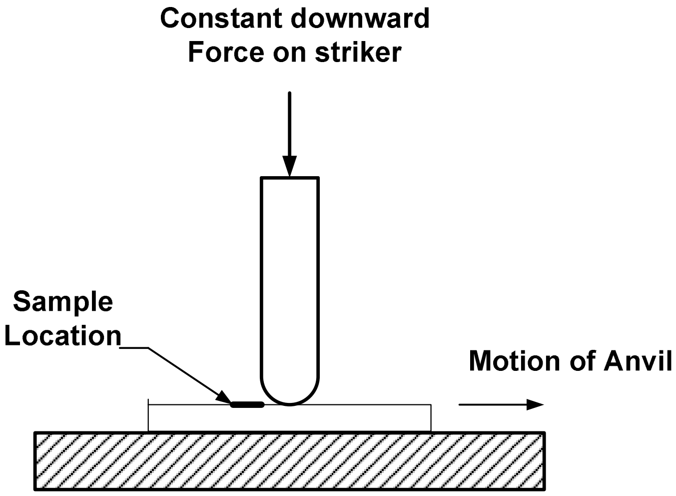

Figure 2.13: Friction sensitivity tester

2.6.2 Impact sensitivity

Impact sensitivity is a measure of a material's tendency to ignite in response to energy input as an impact. As shown in Figure 2.14, a sample is placed between two steel anvils. A drop-hammer is allowed to fall on the upper anvil, which transfers the impact to the sample.

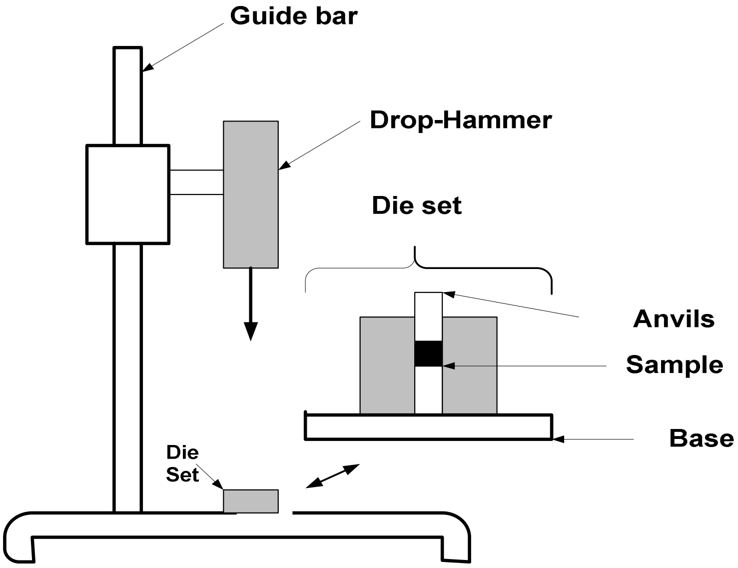

Figure 2.14: Impact sensitivity tester

Impact sensitivity is reported as the height of the drop-hammer that results in ignition (in some specific percentage of 30 trials). Generally, 2 kg and 5 kg drop-hammers are used. Often the surface of the anvil in contact with the sample is about 0.5 cm^2. Because of differences in test methods, it is not unusual to find a range of values reported for the same pyrotechnic material.

2.6.3 Electrostatic sensitivity

Electrostatic sensitivity is a measure of a material's tendency to ignite in response to energy input as an electric spark.

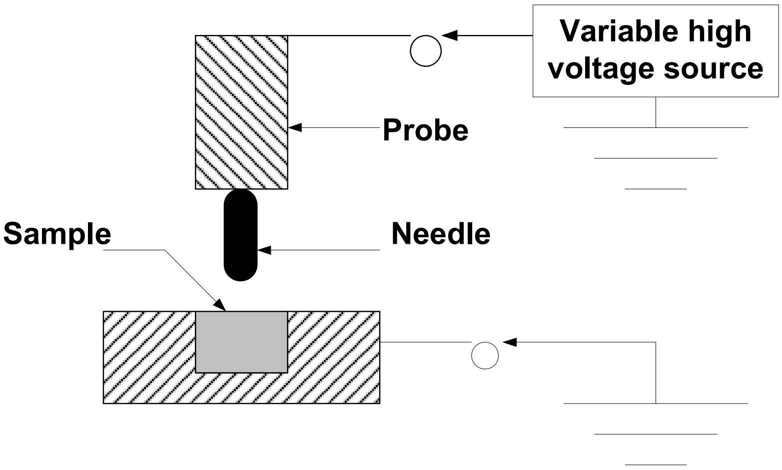

Figure 2.15: Electrostatic sensitivity tester

As shown in Figure 2.15, a sample is placed in a small well in an electrically grounded plate. A probe, connected to a high-voltage power source (usually a charged capacitor), is brought towards the sample until a spark occurs, discharging through the sample. For a given apparatus, electrostatic sensitivity is reported as the electrical energy (in joules) that results in ignition (for some specific percentage of 30 trials). Because of differences in test methods, it is not unusual to find a range of values reported for the same pyrotechnic material.

2.6.4 Auto-ignition temperature

Auto-ignition temperature (the Heat in FISH) is the temperature to which a small sample of pyrotechnic composition must be heated to cause it to ignite spontaneously. Figure 2.16 shows a simple screening test apparatus using a thermocouple gauge to measure temperatures; a stopwatch may be used to determine the time to ignition.

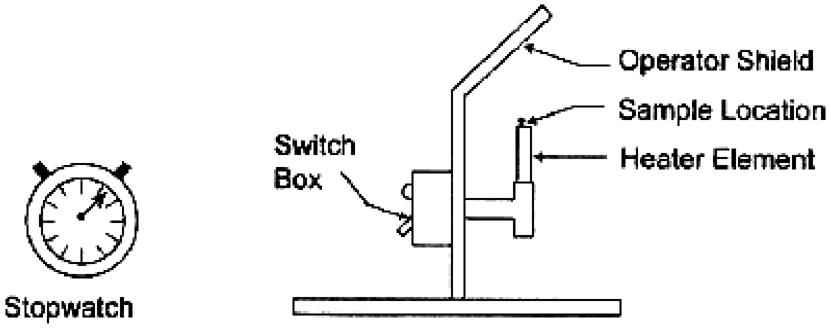

Figure 2.16: Auto-ignition temperature tester

2.7 Thermodynamic considerations for solid-solid state reactions

There are a number of thermodynamic factors involved in the choice of a reducing agent for a particular oxide: Gibbs free energy, the adiabatic flame temperature and the rate of reaction.

2.7.1 Gibbs free energy

Gibbs has shown that the spontaneity of a chemical reaction, at constant temperature and pressure, is determined by the Gibbs free energy (equation (5)).

$$\Delta G = \Delta H - T\Delta S \qquad (5)$$

Consider the chemical reaction below:

$$aA + bB \ = \ pP + qQ \qquad (6)$$

The sign of Gibbs free energy determines the direction in which the above chemical reaction will proceed spontaneously once initiated. A negative value of Gibbs energy ($\Delta G < 0$) indicates that the forward reaction from left to right in the above chemical reaction is favourable. A positive value ($\Delta G > 0$) indicates that the reverse reaction from right to left is favourable and a zero ($\Delta G = 0$) value is a criterion for equilibrium.

From equation (5) it can be noticed that temperature influences contribution of entropy to reaction spontaneity. When the temperature is low, the term $T.\Delta S$ will be small, and consequently the contribution of entropy to spontaneity will be small.

At very high temperatures, the contribution of entropy is large. Thus if enthalpy and entropy make opposite contributions to the free energy, there should be a temperature below which the term $T.\Delta S$ is small enough for the enthalpy term to dominate and above which the entropy term dominates. Thus, chemical reaction is spontaneous when both the enthalpy change has a large negative value and the entropy change has a large positive value

In the solid-solid state reaction between Al and CuO yielding solid products, the aluminium and copper oxidation reactions are:

$$2Cu + O_2 = 2CuO \qquad (7)$$

$$4/3\ Al + O_2 = 2/3\ Al_2O_3 \qquad (8)$$

The reduction reaction of copper oxide by aluminium is expressed by:

$$2\ CuO_{(s)} + 4/3\ Al_{(s)} \rightarrow 2Cu_{(l)} + 2/3\ Al_2O_{3\ (s)} \qquad (9)$$

Note that the net reaction is obtained by adding the 'reverse' of the first reaction (7) to the second reaction (8). Oxygen appears on both sides and cancels out.

The entropy change (ΔS) of the reaction (equation (9)) will be quite small since no gaseous products or reactants are involved (Wilson and Hancox, 2001). So, the only possibility for ΔG to be negative and large according to equation (5) is that $\Delta H < 0$. Therefore the solid-state reaction between Al and CuO must be exothermic (ΔH_r = -1 203.8 kJ/mol).

However, during combustion some constituents remain in the solid state, while others melt, vaporise or decompose to yield some gaseous products. The mechanisms encountered may consequently cover the wide field of solid-solid, solid-liquid, solid-gas and possibly even liquid-liquid or liquid-gas reactions (Brown, 2001). As a general rule, entropy follows the sequence $S_{solid} < S_{liquid} << S_{gas}$ (Conkling, 1985).

2.7.2 Ellingham diagrams

The Ellingham diagrams plot the standard free energy of a reaction as a function of temperature (Figure 2.17). The graph consists of lines of Gibbs free energy change (equation (5)).

Although ΔS and ΔH vary with temperature, the changes are so small as to be negligible, and so the lines are approximately straight. This means that they are of the form: $y = m\ x + c$.

Consider the following reactions on the Ellingham diagram illustrated in Figure 2.17: the oxidation of Al to form $Al_2O_{3(s)}$; and the oxidation of Cu to form $CuO_{(s)}$ and of Si to form $SiO_{2(s)}$:

$$2Cu_{(s)} + O_{2\ (g)} = 2CuO_{(s)}$$

$$Si_{(s)} + O_{2\ (s)} = SiO_{2\ (s)}$$

$$4/3\ Al_{(s)} + O_{2\ (g)} = 2/3\ Al_2O_{3\ (s)}$$

It can immediately be seen that the standard free energy change is greater (more negative) for the aluminium reaction relative to that of silicon and even more for copper at all temperatures. This means that at all temperatures the equilibrium constant is larger for the aluminium reaction (the composition is further weighted towards the products of the reaction). This is the reason that metals that appear higher up on the diagram are more stable than those that appear lower down and are more likely to be found in their pure solid (or liquid) form (equation (9)).

The gradient of the two lines (Al and Si) is approximately the same. The gradient of the lines is simply the standard entropy change for the reactions:

$$\frac{\partial \Delta G^\circ}{\partial T} = -\Delta S^\circ \tag{10}$$

This is evident from the reactions, which both involve the elimination of one mole of gas (a large decrease in entropy). This is the reason for the positive slope of the lines. The reason for the change in slope is the change in phase of a component of the system, which alters the entropy change.

As the standard free energy change for both reactions is still negative, the large decrease in entropy must be counteracted by a large enthalpy of reaction. This is indeed the case. The intercept at 0 K of the tangent line to the ΔG vs temperature curve gives the enthalpy of the reaction:

$$\Delta G^\circ\big|_{0K} = \Delta H^\circ \tag{11}$$

The relative stability of the oxide of aluminium compared with the copper oxide is due to the much larger standard enthalpy of reaction.

Therefore, the Ellingham diagrams may be used in pyrotechnics as a quick check for possible exothermic reaction between compounds such as oxides or sulphides with a specific fuel. A fuel $M_{(2)(s)}$ (e.g. Al) may be a reducing agent with respect to a particular oxide compound $M_{n(1)}O_{m(s)}$ (e.g. CuO) when the Gibbs free energy change for its oxidation is more negative than the Gibbs free energy change of oxidation of the pure metal M $_{(1)}$ (e.g. Cu) (Hannay, 1976).

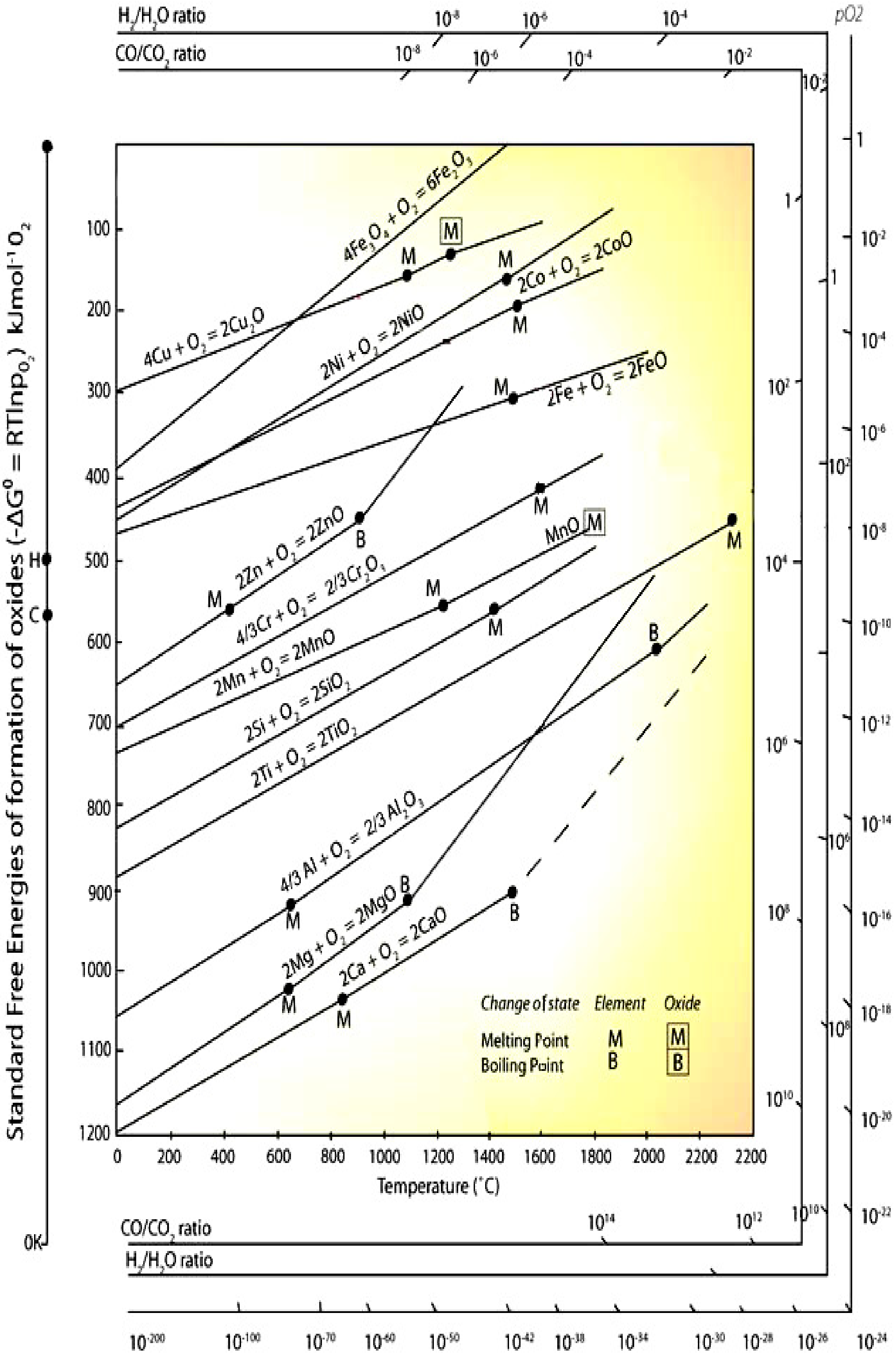

Figure 2.17: Ellingham diagrams

2.7.3 Heat of solid-solid state reaction

The solid-solid state reaction is exothermic, provides its own oxygen supply and is self-sustaining once initiated. The heat of the solid-solid state reaction (ΔH_r), at stoichiometric ratio, is calculated from the enthalpies of formation (equation (12)).

$$\Delta H_r = \Sigma\, n_p\, \Delta\, H_f^{\circ}\ \text{(products)} - \Sigma\, n_r\, \Delta\, H_f^{\circ}\ \text{(reactants)} \qquad (12)$$

The determination of the heat of reaction is simply an exercise of stoichiometry; the required energy properties can be obtained by adjusting the ratio of the reagents (oxidiser and fuel). Figure 2.18 shows the heat of the Al-CuO reaction calculated using different aluminium contents.

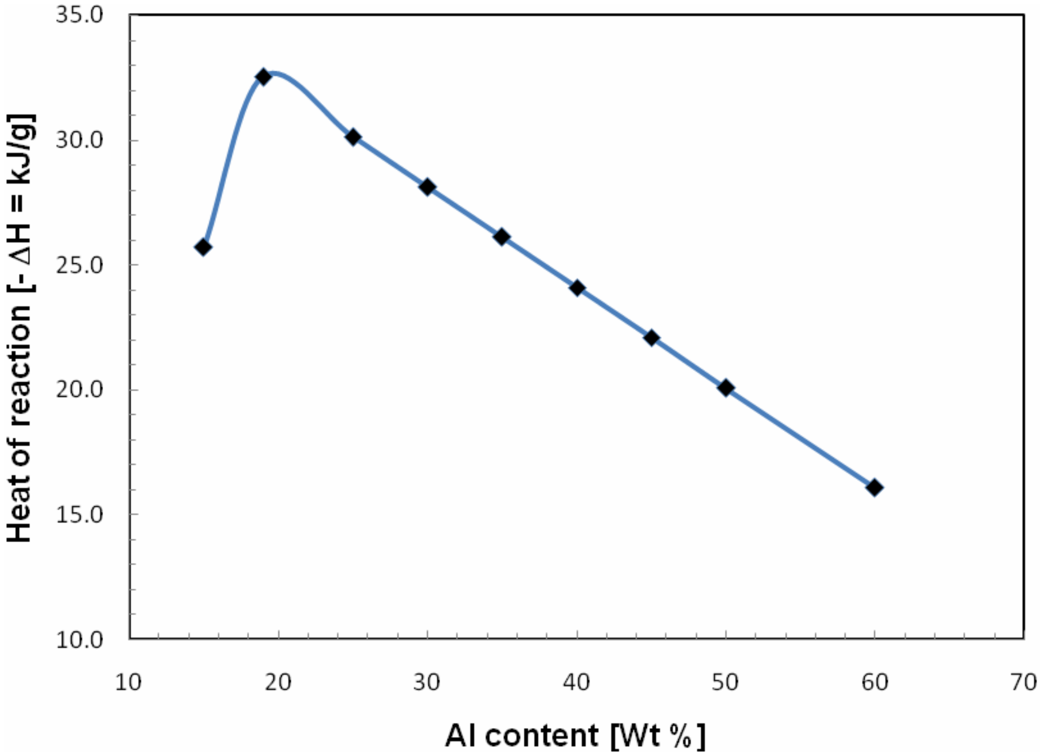

Figure 2.18: Heat of Al-CuO reaction at different aluminium contents

2.7.4 Rates of solid-solid state reactions

Even if the value of the enthalpy changes for a solid-solid state reaction is large and a negative number, there is no guarantee that the reaction will progress rapidly. The rate of reaction is determined by the magnitude of the required activation energy, and it is a temperature-dependent phenomenon. The equation describing this rate-temperature relationship is called the Arrhenius equation.

$$K = A \exp(-E_a/RT) \tag{13}$$

When the natural logarithm of both sides of the above equation is taken, the Arrhenius equation becomes:

$$\mathit{ln}\, k = \mathit{ln}\, A - E_a/RT \tag{14}$$

According to equation (13), the rate at which a chemical system reacts to form products increases exponentially as the temperature of the system is increased. This equation is of considerable importance in the ignition of pyrotechnics and explosives (Conkling, 1985).

2.7.5 Adiabatic reaction temperature

When a combustion process is conducted adiabatically, all the heat liberated by a reaction goes into heating up the products of reaction, with no heat transfer loss to the surroundings. The final temperature achieved by the product of combustion is defined as the adiabatic reaction temperature T_{ad}. This represents the maximum temperature that the products of reaction can achieve if the reaction is conducted both stoichiometrically and adiabatically. According to this condition, all the energy liberated on combustion at or near standard conditions ΔH°_{298} appears as sensible heat ΔH_p in heating up the products of reaction (Oxtoby and Nachtrieb, 1986). This is an application of Kirchhoff's rule and can be represented by the following equation (15):

$$\Delta H^{\circ}_{298} + \Delta H_p = 0 \tag{15}$$

In the final state, all the constituents have reacted and the heat of reaction has gone entirely toward heating the products of reaction, then, slightly, the walls of the vessel. Therefore:

$$\Delta H_p = \Sigma\, C_p\,(T_p - T_a) \tag{16}$$

Where $\sum C_p$ is the summation of the respective numbers of moles of the products multiplied by the corresponding values of C_p.

This equation can be rearranged as in equation (17):

$$T_{ad} = (-\Delta H^\circ_{298} / \Sigma C_p) \tag{17}$$

If the heat capacity of products is weakly dependent on temperature, T_a and $\sum C_p$ are constants, then the above equation shows that T_{ad} increases linearly with $-\Delta H^\circ_{298}$.

But in reality, the above equation must be used carefully. Firstly, the temperature changes involved are often very large and the C_p is not constant. Secondly, at high temperatures a component can undergo phase changes during the combustion process. These transitions can remove some of the heat originally produced and lead to a maximum temperature that is often lower than the predicted one (Oxtoby and Nachtrieb, 1986).

The heat capacity of each product of reaction can be expressed as a polynomial expression with temperature as variable (Kubaschewski *et al.*, 1993). As the temperature increases from ambient temperature to the theoretical adiabatic temperature, the enthalpy change of the products can be estimated by equation (18).

$$\Delta H_p = \int_{298}^{T} \Sigma C_p dT \tag{18}$$

For reactions involving phase transitions, the adiabatic temperature of the components is evaluated from equation (19) (Hannay, 1976):

$$-\Delta H_{298} = \int_{298}^{Ti} C_p\,(\alpha) dT + \Delta H_{Ti} (\alpha = \beta) + \cdots + \int_{Tk}^{Tad} C_p\,(\gamma) dT \tag{19}$$

Fischer and Grubelich (1993) applied equation (19) to some selected thermite compositions to determine the adiabatic reaction temperatures; the results are given in Table 2.2.

Table 2.2: Heat of reaction, adiabatic reaction temperature, and state of the product metal and oxide of selected thermite reactions (Fischer and Grubelich, 1998)

Thermite reaction	Q (MJ/kg)	T_{ad} (°C)	State of product	
			Oxide	Metal
$2Al + Fe_2O_3 \rightarrow 2Fe + Al_2O_3$	3.96	2 862	liquid	liquid-gas
$2Al + Bi_2O_3 \rightarrow 2Bi + Al_2O_3$	2.11	3 046	liquid-gas	gas
$2Al + 3CuO \rightarrow 3Cu + Al_2O_3$	4.08	2 570	liquid	liquid-gas
$4Al + 3MnO_2 \rightarrow 3Mn + 2Al_2O_3$	4.85	2 645	liquid	gas

2.8 Propagation of Pyrotechnic Compositions

Even when a portion of a pyrotechnic composition has been ignited, propagation (burning throughout) is not guaranteed. Heat is produced by the burning composition (reacting material). A fraction of that heat is transferred to the surroundings (e.g. air, unburned composition, etc.). If enough heat is transferred to the next layer of unreacted composition (pre-reacting material) to raise it to the ignition temperature, burning will continue (propagate).

2.8.1 Types of energetic powder confinement

The type of burning that occurs depends on whether gases are produced and on the physical form of the pyrotechnic material: compacted solid or loose granular as shown in Figure 2.19.

Loose powders

When a container filled with a loose pyrotechnic powder is initiated, the burning speed of the reaction is uncontrollable (propagative burning). The low bulk density of the material permits heat transfer by convection of gaseous products; gas occlusions that are present in the original powdered mixture undergo heating, accompanied by a rise in pressure. The propagation zone will accelerate rapidly through a loose collection of such powder (Conkling, 1985). For loose thermite compositions, the burning speed can reach a detonation velocity.

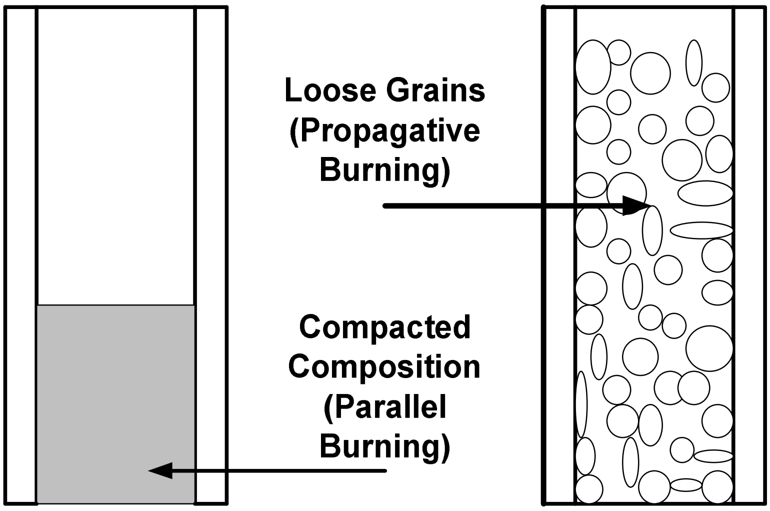

Figure 2.19: Types of pyrotechnic confinement and burning

Compacted powders

In contrast to a loose pyrotechnic powder, a compacted powder does not permit much motion of combustion products through voids. Heat transfer is achieved by conduction. Combustion occurs within a relatively thin propagation zone (parallel burning) known as the 'burning front'. For 'gasless' pyrotechnic compositions factors such as the time delay or a rise in loading pressure should lead to an increase in the burn rate. This is due to more efficient heat transfer via closely compacted solid and melted particles (Conkling, 1985).

2.8.2 Shimizu diagrams

Figure 2.20 represents, in general, Shimizu diagrams (Kosanke *et al.*, 2004) where E_a is the activation energy, E_f is the energy feedback, and F_{fb} is the fraction of energy fed back. The energy feedback is the amount of energy produced by a pyrotechnic composition that is fed back to the unburned composition. This may be represented by equation (20):

$$E_f = \Delta H_r . F_{fb} \tag{20}$$

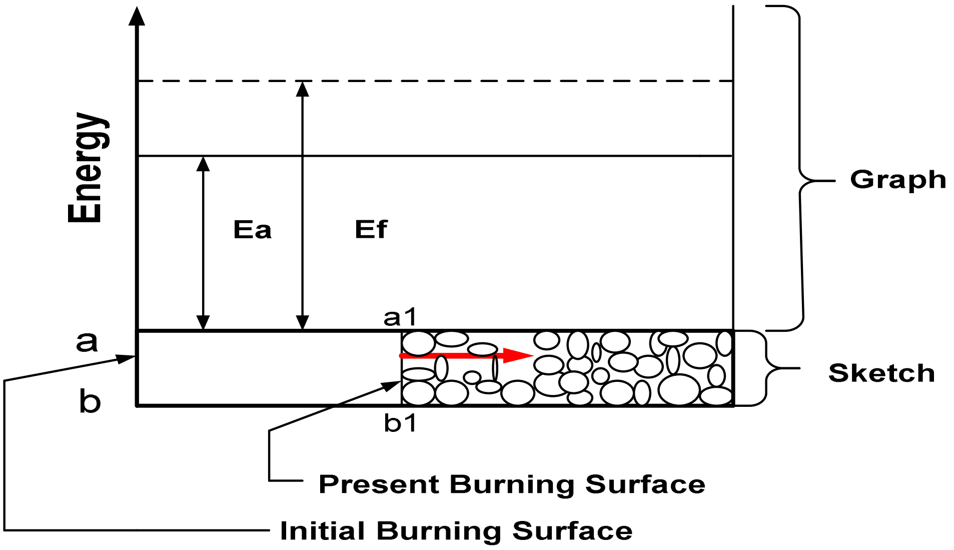

Figure 2.20: Shimizu diagram

- **If $E_f < E_a$:** Composition will not propagate. It may react under heavy ignition stimulus, but will extinguish upon removal of the stimulus.
- **If $E_f \geq E_a$:** Composition will propagate weakly but can be easily extinguished.
- **If $E_f > E_a$:** Composition will propagate vigorously and will be difficult to extinguish.

According to the Shimizu diagrams, the characteristics of a good compacted pyrotechnic composition are:

- Is easily ignited when E_a is low.
- Generates abundant thermal energy (ΔH_r is high).
- Is not overly sensitive to accidental ignition (E_a is not too low).
- Has efficient energy feedback mechanisms (thermally conductive, generates molten slag).

2.8.3 Ranges of parameters for classes of pyrotechnic combustion

Combustion can be roughly divided into three classes: burning, deflagration, and detonation. It is not possible to set precise limits on the values of parameters for the three classes of pyrotechnic combustion. However, approximate ranges are given in Table 2.3.

Table 2.3: Values of parameters of the three classes of pyrotechnic combustion (Kosanke *et al.*, 2004)

Parameter	Burning	Deflagration	Detonation
Burn rate (m/s)	10^{-3}–10 << Sonic	10–2 000 < Sonic	1 500–10 000 > Sonic
Temperature (ºC)	300–3 500	1 500–4 000	2 000–4 000
Unconfined pressure (atm)	1	1–10^{2}	1x 10^{4}–5x10^{5}
Reaction time (s)	1–10^{-3}	10^{-2}–10^{-4}	10^{-6}–10^{-9}
Propagation mechanism	Thermal	Thermal and compression	Shock wave compression
Particle motion	Reverse	Primarily reverse	Primarily forward

2.8.4 Complete model of pyrotechnic burning

A more complete model of burning (Shidlovskiy, 1997) is shown in Figure 2.21.

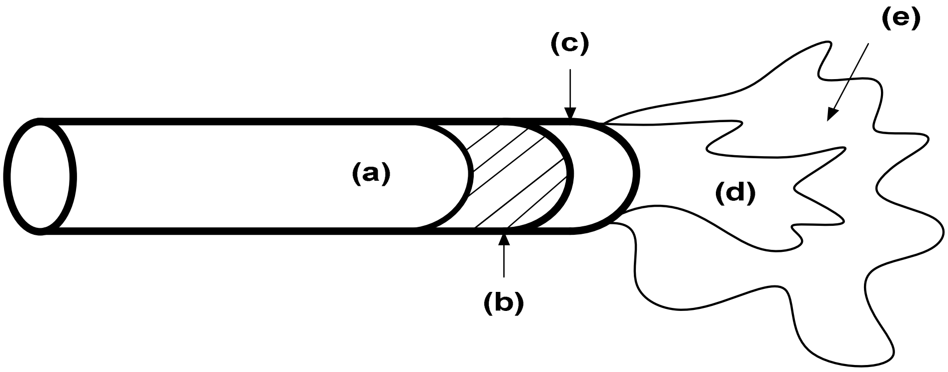

Figure 2.21: Complete model of pyrotechnic burning

(a) Unreacted pyrotechnic composition; (b) warm-up zone (possible solid-state reactions); (c) reaction in condensed phase (at least one liquid phase); (d) reaction in gaseous phase (liquid droplets possible); and (e) reaction complete, combustion products are cooling

The temperature profile of the complete model of propagation is also shown in Figure 2.22 below.

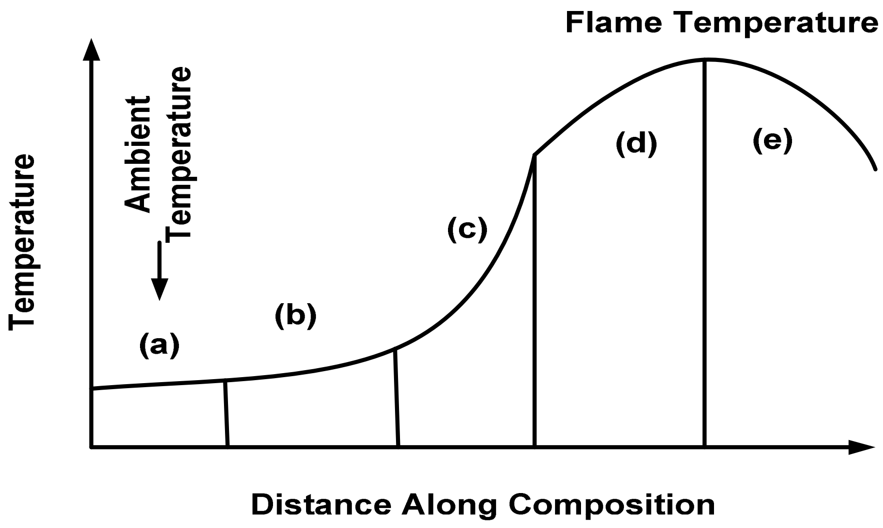

Figure 2.22: Temperature profile of pyrotechnic propagation

There are two basic types of pyrotechnic burning, as shown in Figure 2.23.

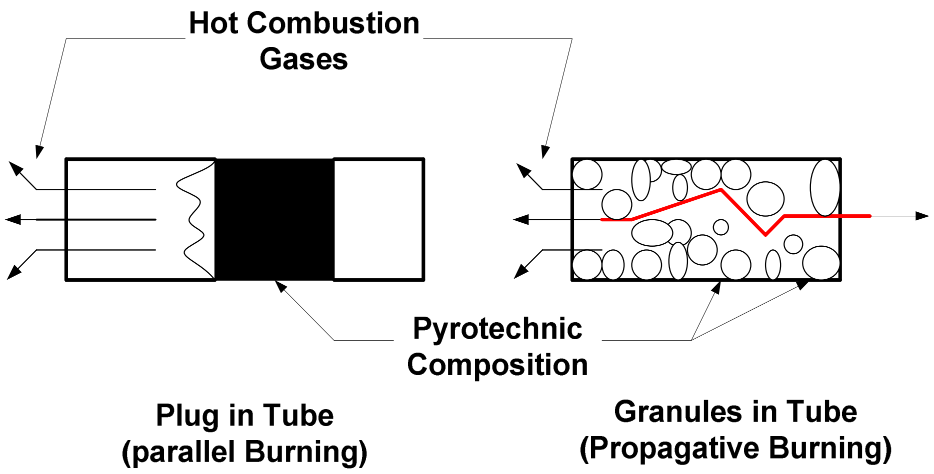

Figure 2.23: Two basic types of propagation: plug in tube and granules in tube

- **Parallel burning:** Burning occurs layer by 'parallel' layer until all material is consumed.

- **Propagative burning:** Each individual granule experiences parallel burning but, because of penetration of hot combustion gases along 'fire paths', the burning 'propagates' rapidly throughout the entire mass of composition.

2.8.5 Simplified model of propagation

Figure 2.2.4 shows a simplified model of propagation for the parallel burning of pyrotechnic compositions.

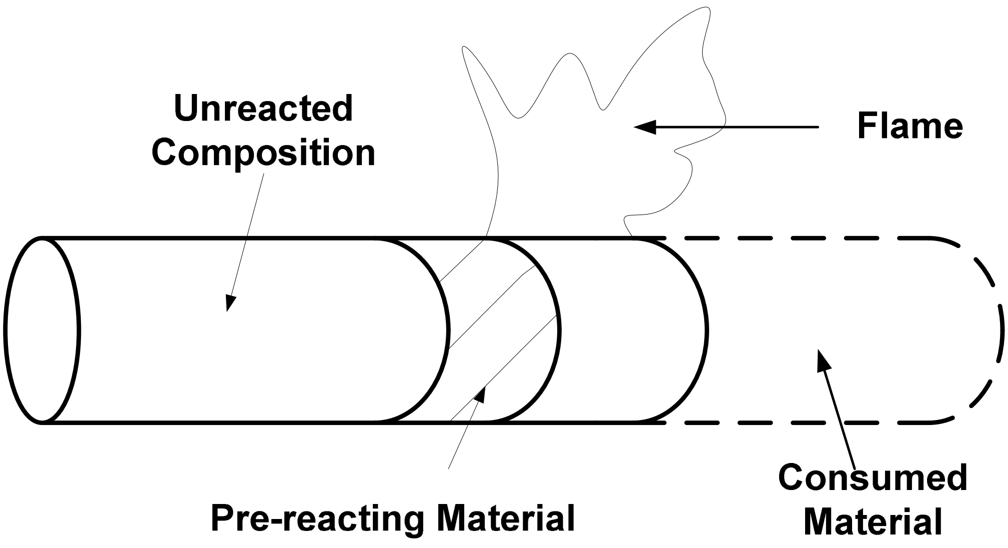

Figure 2.24: Simplified model of pyrotechnic burning

Once a pyrotechnic composition is ignited, there is a rapid and exothermic reaction in the area of the reaction sites. The combustion process occurs by deflagration; the heat generated from the locally ignited region can subsequently trigger reaction in the adjacent reactant layer when the ignition temperature is low (layer-to-layer propagation). Thus, the reaction zone moves in the form of a wave until all the reactants have been consumed (Crider, 1982), as shown Figure 2.25.

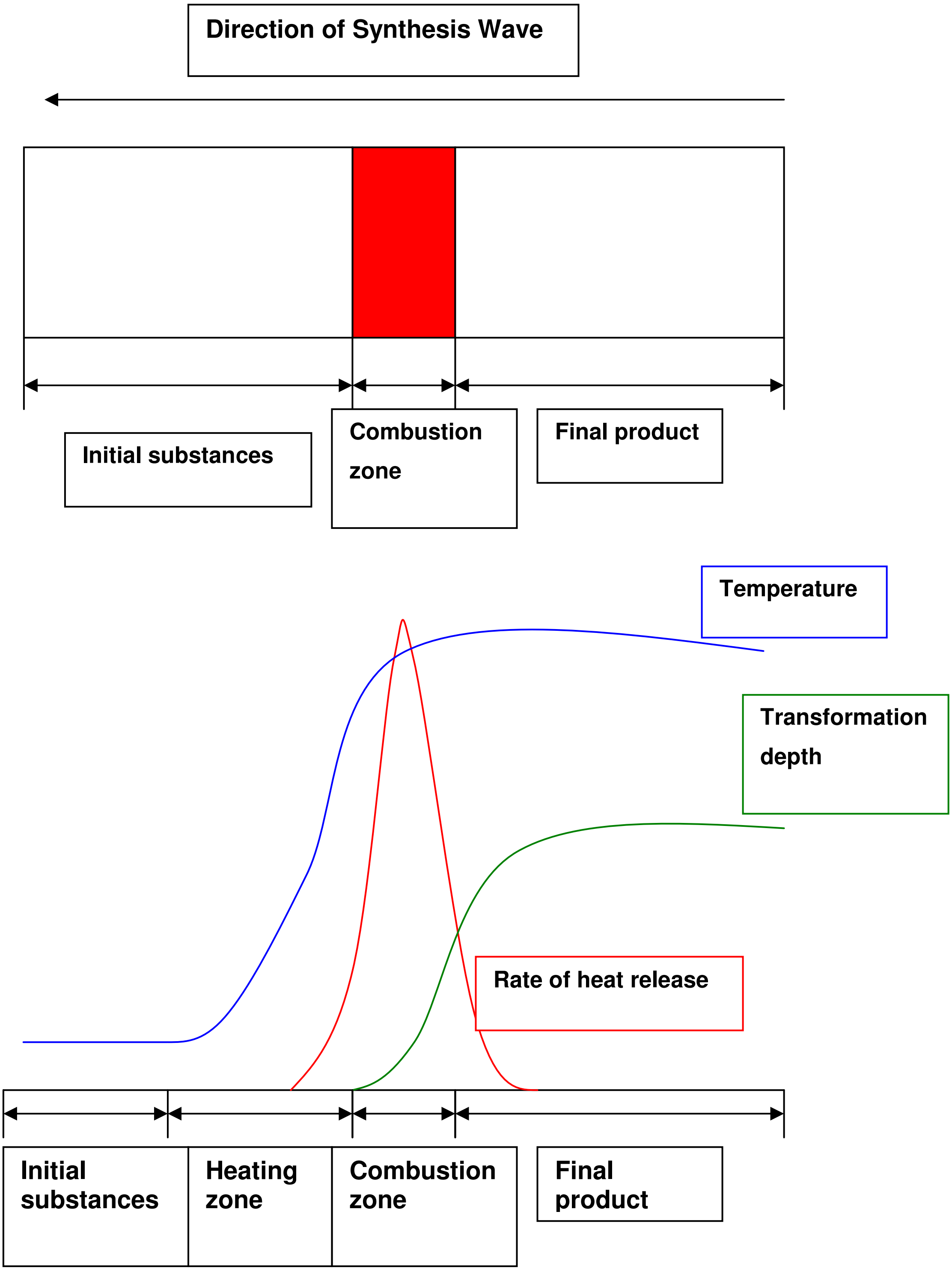

Figure 2.25: Simplified diagram of an equilibrium combustion wave (Crider, 1982)

2.9 Burn Rate of Pyrotechnic Compositions

Once a pyrotechnic composition is initiated, there is a rapid and exothermic reaction in the area of the reaction sites. The combustion process occurs by deflagration; the heat generated from the locally ignited region can subsequently trigger the reaction in the adjacent reactant layer when the ignition temperature is low (Booth, 1958). Thus, the reaction zone moves in the form of a wave until all the reactants are consumed (Crider, 1982).

From layer-to-layer burning theory, an equation was derived which gives the uniform velocity u of the reaction zone along the pyrotechnic column (Khaikin and Merzhanov, 1966).

The following assumptions were made:

- No transfer of heat due to radiation (or reaction); gas is not involved gas the burning process.
- The problem is regarded as one-dimensional.
- Loss of heat from the side of the rod is neglected.
- Thermal conductivity, specific heat and density of the powder material are constants.

After derivation, it follows that:

$$u = \sqrt{\exp\left(-\frac{E_a}{RT_c}\right) g(n) \frac{\lambda . k_0 R T_c^2}{\rho E_a \Delta H_R}} \tag{21}$$

Where

u is the burn rate (m s^{-1})

λ is the thermal conductivity (Wm^{-1} K^{-1})

ρ is the density (kg m^{-3})

R is the gas constant (8.314 J mol^{-1} K^{-1})

T_c is the maximum temperature of the burning column

E is the apparent Arrhenius activation energy (J mol^{-1})
$\Delta_R H$ is the heat of reaction (J kg^{-1})
k and k_o are the rate constant and Arrhenius pre- exponential factor ($s^{-}1$)
g(n) is a weak function of the reaction order n which varies between 1 and 2.

From equation (21), the following laws can be immediately deduced:

- The more relatively high the thermal conductivity (e.g. metallic fuel) of the mixture is, the more rapid is the burning velocity.
- The reaction temperature T_c is the most significant factor affecting the burn rate. Instability of the combustion wave can come from insufficient heat generated, due to weak exothermic reactions (Munir, 1988).
- The loading pressure has an effect on the burn rate:

In essence, the burn rate of a pyrotechnic composition is determined by how quickly the pre-reacting layer of composition can be raised to its ignition temperature. The factors that control burn rate are those things that affect (Kosanke *et al.*, 2004):

- activation energy (E_a)
- heat of reaction (ΔH_r)
- efficiency of thermal energy feedback (E_f).

2.9.1 Mechanisms for controlling the burn rate

The burn rate of a pyrotechnic composition may be adjusted through the control mechanisms listed in Table 2.4.

Table 2.4: Mechanisms for controlling the burn rate (Kosanke *et al.*, 2004)

Control mechanism	Effect on burn rate
Lowering E_a	Higher burn rate
Raising ΔH_r	Higher burn rate
Increasing feedback	Higher burn rate
Raising E_a	Lower burn rate
Lowering ΔH_r	Lower burn rate
Decreasing feedback	Lower burn rate

The factors affecting the efficiency of energy feedback are directly related to the three mechanisms for conveying thermal energy as listed in Table 2.5 (Kosanke *et al.*, 2004).

Table 2.5: Transfer mechanisms influencing feedback efficiency

Transfer mechanism	High feedback efficiency
Convection	Many fire paths
Radiation	Black or dark composition
Conduction	Metal fuels and compaction

2.9.2 Factors affecting the burn rate

According to Kosanke *et al* (2004), there are a number of factors that affect the burn rate.

Effect of choice of chemicals on the burn rate

The chemicals chosen can affect all three factors controlling the burn rate.

- Activation energy differences

  $KClO_3$ – exothermic decomposition (low E_a)
  KNO_3 – endothermic decomposition (high E_a)

- Heat of reaction differences for combustion

  Al: $\Delta H_r = 7.4$ kcal/g (high)
  S: $\Delta H_r = 2.2$ kcal/g (low)

- Energy feedback differences

  Metals – high thermal conductivity
  Non-metals – low thermal conductivity

Consequently:

$KCl0_3$ + Al: high burn rate
KNO_3 + S: low burn rate (barely burns)

Effect of fuel-to-oxidiser ratio on the burn rate

There is always an optimum fuel-to-oxidiser ratio that generates a fast burn rate. As this ratio varies from the optimum ratio (that required for complete burning), the burn rate generally decreases because the excess fuel or oxidiser fails to contribute any energy (i.e. the heat of reaction is reduced). It could also be thought of as consuming energy because the excess material (not being utilised) must be heated along with the rest of the composition. The activation energy may change because of changes in the heat capacity and ignition temperature of the composition. The efficiency of the energy feedback can change as a result of changes in the physical properties of the composition as the fuel-to-oxidiser ratio changes.

Effect of mixing on the burn rate

Before being well mixed, most of the material will be at far from the ideal ratio, and the burn rate will be quite low. In essence, although the entire volume of the poorly mixed pyrotechnic composition may have the optimum fuel-to-oxidiser ratio, there will be many small regions where this ratio is far from optimum. As the degree of mixing increases, the burn rate increases towards its maximum value. Incorporation is the process of bringing fuel and oxidiser into more intimate contact. Figure 2.26 shows an example of the incorporation of black powder.

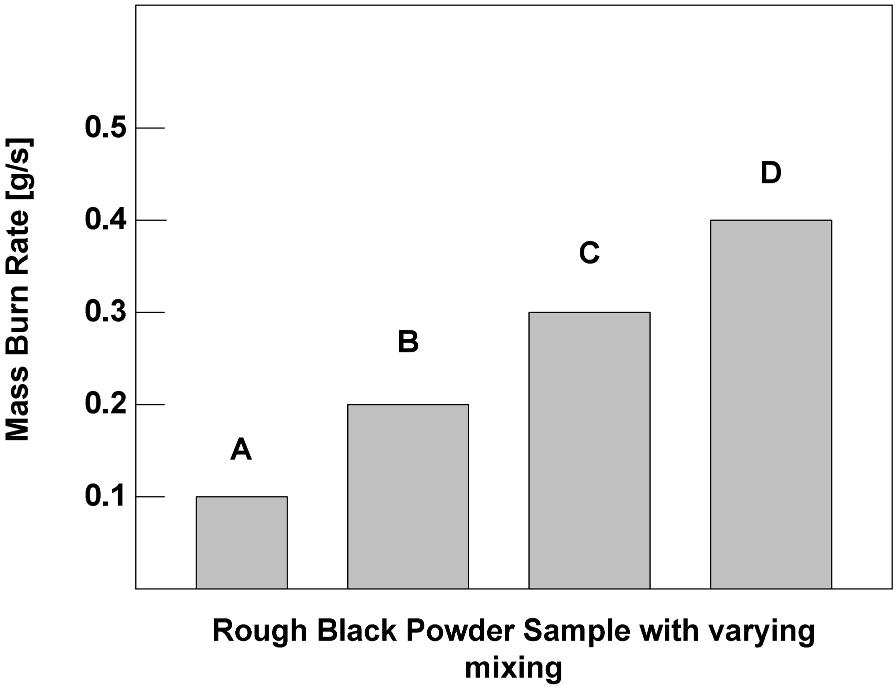

Figure 2.26: Mass burn rate of black powder resulting from different incorporation processes

A = dry mixed several times through a 60 mesh screen; B = wet mixed for several minutes with a mortar and pestle; C = wet ball-milled for 4 hours, dried and crushed to 100 mesh; D = fuel dry ball-milled for 4 hours, oxidiser added and wet ball-milled for 8 hours, dried and crushed to 100 mesh

Effect of particle size on the burn rate

As the particle size of the individual fuel and oxidiser is reduced, the burn rate increases. This is because small particles are more easily heated during the reaction due to the reduction of the effective activation energy. In addition, the fraction of atoms that are on the surface of particles increases as size decreases. This can also be thought of as the result of a particle's surface-to-mass ratio. Small particles with a high surface-to-mass ratio are more reactive. The particle size effect is most noticeable for fuels; oxidisers usually have started to melt (or have melted) before the ignition temperature is reached.

Effect of particle shape on the burn rate

Particle shape affects the burn rate in much the same way as particle size. Spherical particles do not heat quickly (have a relatively low surface-to-mass ratio). Thus they have relatively high activation energy. Flakes are at the other extreme, producing compositions with the lowest activation energy. Particle shape is most important for fuels because oxidisers usually have started melting before ignition.

When molten aluminium is sprayed into an atmosphere containing oxygen, a crust of Al_2O_3 quickly forms, causing the particle to assume highly distorted shapes. Flake aluminium is made by milling other particle shapes. The impacts during milling will cause the flakes to stick together, unless a lubricant is added.

Effect of additives on the burn rate

Pyrotechnic additive is material added to a composition for achieving a specific pyrotechnic effect or purpose. Binders, including the residual solvent used to activate a binder, are common examples of additives. Most additives lower the burn rate by either increasing the activation energy E_a or reducing the heat of reaction ΔH_r. However, some additives may increase the burn rate, generally by raising the heat of reaction ΔH_r or increasing the fraction of energy fed back F_{fb}. Additives may consume energy (heat) in their decomposition or elimination.

Additives may function as a fuel or oxidiser; however, they may produce less energy than the principal fuel or oxidiser. The presence of these additives lowers the overall heat of reaction for the composition and, therefore, generally lowers the burn rate as well.

Effect of burn rate modifiers on the burn rate

A burn rate modifier is an additive used for the primary purpose of adjusting the burn rate (up or down). A burn rate modifier can act to reduce the burn rate, as described for typical additives. It can also act to increase the burn rate. This will be the case if it increases the heat of reaction or if it increases the efficiency of thermal energy feedback.

Examples of burn rate modifiers used in pyrotechnic compositions are:

- **Zirconium powder:** Increases the heat of reaction (there is some increase in the conductive feedback efficiency).
- **Lampblack:** Increases the radiant energy feedback efficiency.

Effect of catalysts on the burn rate

Burn catalysts often act by reducing the activation energy by lowering the decomposition temperature of an oxidiser. This lowers the ignition temperature and increases the burn rate because less time is required to reach the now lower ignition temperature (Figure 2.9).

Effect of ambient temperature on the burn rate

Ambient temperature is the temperature of the surroundings; normally, it is also the temperature of the unreacted composition. As the ambient temperature rises, the activation energy is lowered because less energy is needed to raise a composition to its ignition temperature. Thus as a stick of pyrotechnic composition burns, the burn rate is increased because less time is required to reach the ignition temperature of each successive thin layer of pyrotechnic composition.

Effect of compaction on the burn rate

Increasing the loading pressure, i.e. the pressure applied when compacting a pyrotechnic composition, increases the compaction. This increases the thermal conductivity, but closes the ‘fire paths’, as shown in Figure 2.27.

The effects can be explained as follows:

- **When no gas is produced upon burning:** Increases in loading pressure increase the thermal conductivity, which generally increases the burn rate.

- **When gases are produced upon burning (true for essentially all fireworks compositions):** Increases in loading pressure reduce the gas penetration into the unburned composition, which generally decreases the burn rate.

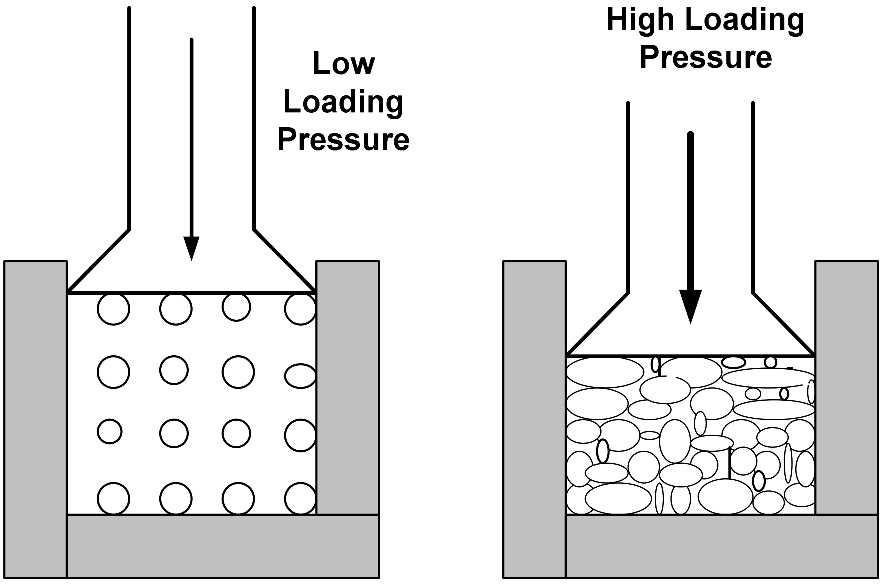

Figure 2.27: Effect of loading pressure on powder density

Furthermore, when increments of powder are compacted, the effective loading pressure varies with distance through the increment, as shown in Figure 2.28. The material closest to the ram is the most compacted. Because of this variation in compaction, it is generally felt that the approximate height of each increment should be not greater than the inside diameter of the tube.

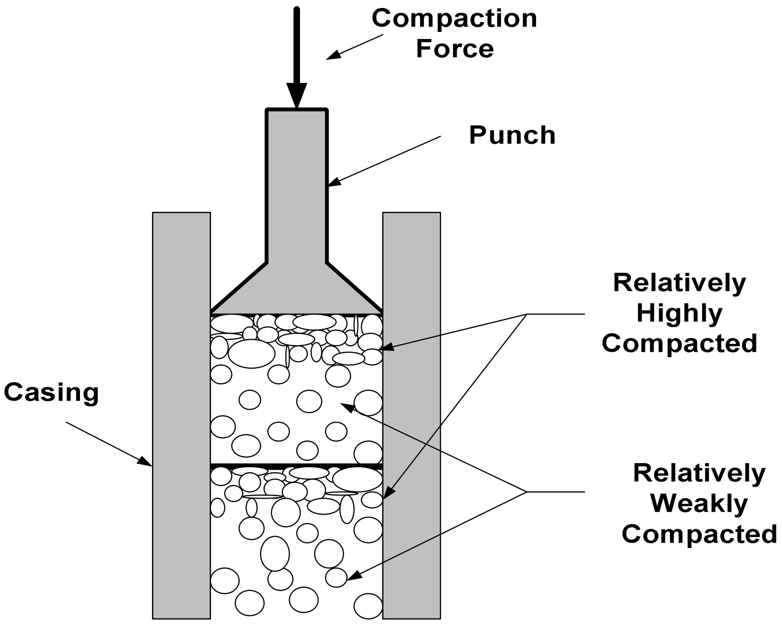

Figure 2.28: Variation of loading pressure with distance

Effect of physical form on the burn rate

The physical form of the pyrotechnic composition can make a great difference to its burn rate. Mostly this affects the efficiency of energy feedback. For a gas-producing pyrotechnic composition, granulated compositions (with so-called 'fire paths') have higher burn rates. Large solid masses of composition (with no fire paths) have low burn rates. Fine powders can have highly unpredictable burn rates; of the three feedback mechanisms, convective energy feedback is the most important here. In the case of granulated materials, where fire paths exist, the hot burning gases produced by the reaction can penetrate rapidly between the grains into the unreacted composition, igniting more material in the process and producing burning gas, thus penetrating further in an accelerating process. In this way all of the pyrotechnic composition can come to be ignited quickly.

Effect of confinement on the burn rate

If a pyrotechnic composition is under confinement, the activation energy is not changed and neither is the heat of reaction, unless significantly different products are formed as a result of confinement. Burning of gas-producing pyrotechnic compositions under confinement can be thought of as burning under conditions where, until the confining vessel bursts, the efficiency of energy feedback is extremely high. During unconfined burning, most of the energy produced is lost to the surroundings as escaping combustion products and radiation. However, when the composition is confined, essentially all the energy being produced is retained and is available to ignite unreacted pyrotechnic material. Also, because the gaseous products are retained, there will be the effect of pressure-accelerated burning. Accordingly, confinement can act to greatly increase the burn rate of gas-producing pyrotechnic compositions. For gas-less pyrotechnic compositions, there is considerably less effect from confinement.

Effect of local pressure on the burn rate

The relationship between the burn rate (V_B, in cm/s) of a pyrotechnic composition and the local pressure (P, in atmospheres) can be expressed mathematically as in equation (22):

$$V_B = A.\ P^B \qquad (22)$$

Where A and B are constants that depend on the pyrotechnic being used. For black powder, the constant A is 1.21 and B is 0.24 (Kosanke *et al.*, 2004).

In conclusion, there are at least 15 factors that can influence (control) the burn rate of pyrotechnic reactions as listed in Table 2.6. More specially, the most important of these effects are the three terms in propagation inequality: Activation energy (E_a), Heat of reaction (ΔH_r), and fraction of energy fed back (F_{fb}).

Table 2.6: Factors influencing the burn rate of pyrotechnic reactions

Controlling factor	**E_a**	**ΔH_r**	**F_{fb}**
Choice of fuel and oxidiser	X	X	X
Fuel to oxidiser ratio		X	
Degree of mixing		X	
Particle size	X		
Particle shape	X		
Presence of additives	X	X	X
Presence of modifiers	X		
Ambient temperature	X		
Local pressure (compaction)			X
Degree of confinement			X
Physical form			X
Degree of consolidation			X
Geometry			X
Crystal effects	X		X
Environmental effects	X	X	X

"X" indicates major control mechanisms

2.10 Energy Properties of Pyrotechnic Materials

The energy properties of pyrotechnic materials are dependent on the nature of the reactants and the stoichiometric balance between oxidiser and fuel in the mixture. However, due to the granular nature of composite energetic materials, reaction kinetics are generally controlled by the mass transport rates between reactants (Valliappan *et al.*, 2005). Thus, the energy release rate of pyrotechnics is lower than what may be attained in a kinetically controlled process such as that with monomolecular energetic materials (explosives).

One alternative way to combine the excellent thermodynamics of composite energetic materials with the rapid kinetics of explosives is to mix the granular components on a nanometre scale which limits the effects of mass transport on the reactants (Tillotson *et al.*, 2001).

During the past few years, significant progress has been made in the synthesis of crystalline nanoparticles of metal oxidisers and in their application in ultra-fast energetic materials (Prakash *et al.*, 2004). An anticipated enhancement in the reactivity of nanoscale metal oxidisers is based on a significant increase in the ratio of surface area to volume. This will provide a tremendous driving force for diffusion, especially at elevated temperatures. The rate of energy release will increase due to there being a shorter diffusion path to limit the reactant (Valliappan *et al.*, 2005).

In addition, as the ratio of surface area to volume increases, the energetic material obtained is both of high energy density (kJ/cm^3) and powerful. Metastable nanoenergetic composites (superthermites), including Al-MoO_3, Al-WO_3, Al-CuO and Al-Bi_2O_3, have been identified as potential substitutes for the currently used primary explosive, lead styphnate (Erickson *et al.*, 2008).

CHAPTER 3 EXPERIMENTAL

3.1 Raw materials

This study considered both micrometre-sized (denoted as ‘micron’ herein) and nano-sized particles (labelled ‘nano’ herein). Scanning electron micrograph (SEM) images of the various powders used are shown in Figure 3.1. The micrometre-sized (**A**) aluminium powder (< 25 µm) used as an energetic fuel was supplied by PAL Chemicals and the nano-sized (**B**) aluminium flakes were supplied by the CSIR. In the latter case the flakes actually feature micrometre dimensions but their thickness was in the range 100 nm to 200 nm. The nano-sized (**D**) silicon powder (< 50 nm, purity > 99%) was obtained from Hefei Kaier. Nano-sized (**F**) CuO (< 50 nm) and (**H**) Bi_2O_3 (< 100 nm, purity > 99.9%) were purchased from Sigma-Aldrich Chemicals. The micron-sized (**E**) CuO was a laboratory-grade powder from Merck that was ground finer by ball milling. The micron-sized silicon was Type 4 (**C**) supplied by Millrox. It had a surface weighted mean particle size of 0.91 µm and a BET surface area of 10.1 m^2/g. Micron Bi_2O_3 was prepared by thermal decomposition of bismuth basic carbonate at 460 °C using the method described by Kalombo *et al* (2007).

The BET surface areas and the particle sizes of the powders used in this study are given in Table 3.1.

Table 3.1: BET surface area and particle size of the powders

Metal	**Al**		**Si**		**CuO**		**Bi_2O_3**	
Size	***nano***	***micron***	***nano***	***micron***	***nano***	***micron***	***nano***	***micron***
BET, m^2/g	4.77	0.39	37.1	9.1	17.6	9.25	2.24	0.37
D0.1, µm	5.12	9.65	-	0.39	-	1.96	-	3.20
D0.5, µm	18.0	24.3	-	1.39	-	5.76	-	13.8
D0.9, µm	48.1	55.2	-	63.6	-	25.5	-	33.6

[redacted]

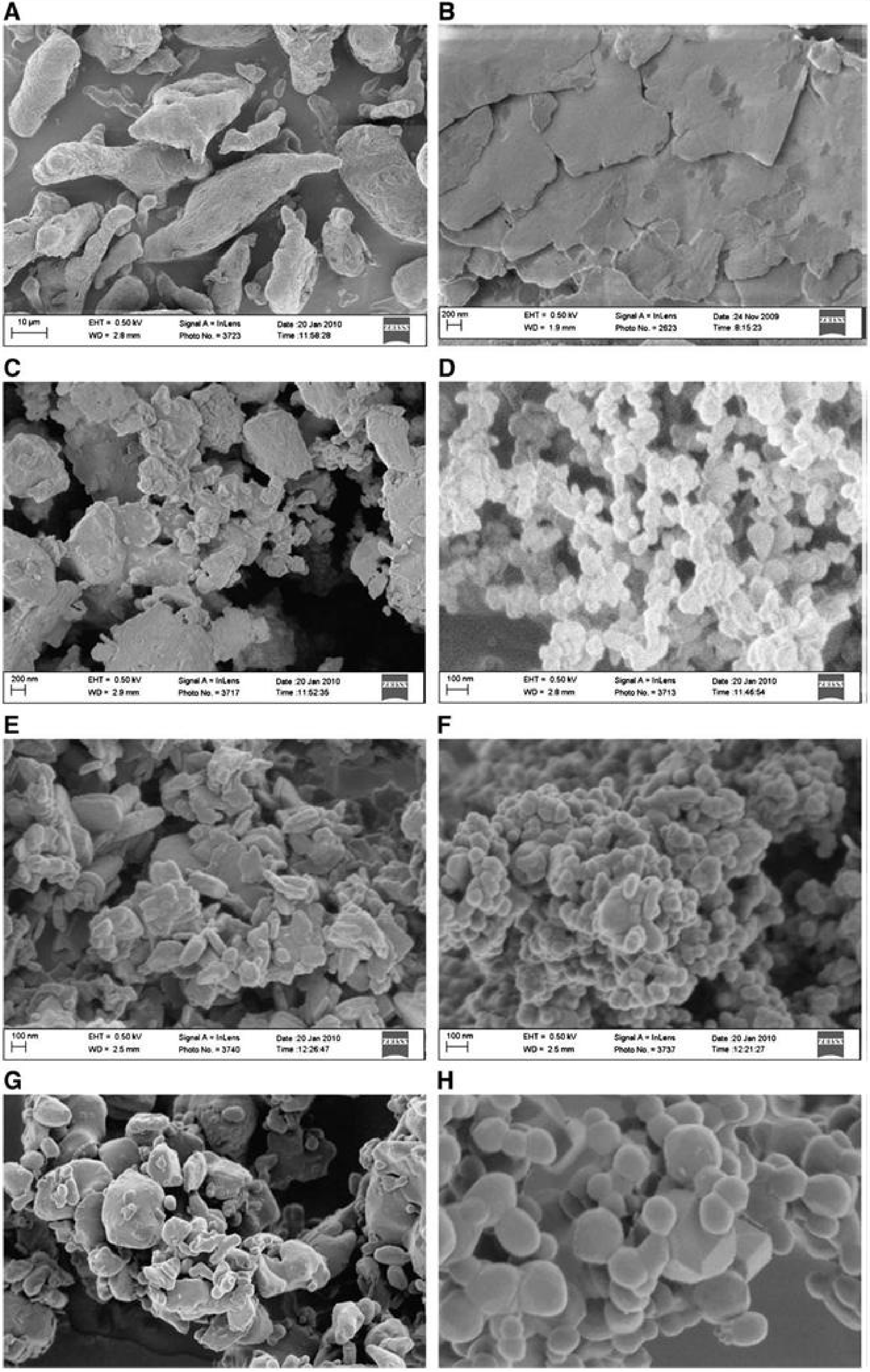

Figure 3.1: SEM pictures of raw materials

The XRD spectra revealed the following: the Si and Al powders were X-ray pure cubic phases. The CuO powders were monoclinic but the nanopowder contained some of the cubic phase and $Cu_2(OH)_3NO_3$ (orthorhombic) as minor impurities. The micron Bi_2O_3 was X-ray pure monoclinic phase but the nano Bi_2O_3 was of the tetragonal phase.

3.2 Characterisation of pyrotechnic materials

3.2.1 X-ray powder diffraction (XRD) analysis

Each crystalline phase has a unique powder diffraction pattern. It is possible to distinguish between compounds as the diffraction method is sensitive to structure and not just composition. Furthermore, it is possible to distinguish between different polymorphic forms of the same compound.

Phase identifications of raw materials were carried out by XRD analysis performed on a PANalytical X'Pert Pro powder diffractometer. The instrument was fitted with an X'Celerator detector and variable divergence and receiving slits with Mn-filtered Fe-Kα radiation (0.193609 nm) operated at 25 kV and 35 mA. The phases were identified using X'Pert Highscore Plus software and the composition was quantified using the Rietveld method.

3.2.2 Scanning electron microscopy (SEM)

A scanning electron microscope is a type of electron microscope that creates various images by focusing a high-energy beam of electrons onto the surface of a sample, and detecting signals from the interaction of the incident electrons with the sample’s surface.

A Field emission scanning electron microscope – FEGSEM JSM-6000F (JOEL, Tokyo, Japan) of high resolution and a scanning electron microscope – JSM-840 (JOEL, Tokyo, Japan) of low resolution were used to investigate the morphology of the raw materials.

3.2.3 Particle size distribution

Single point BET surface area measurements were done using a Coulter SA 3100 instrument. Particle size determinations were performed using a Malvern Mastersizer Hydro 2000MU instrument. Unfortunately, it was not possible to measure the particle sizes of the nano-sized powders.

3.3 Sample preparation

A significant increase in the burning speed of a pyrotechnic mixture is caused by enhanced dispersion and mixing of nanoreactants (Valliappan *et al.*, 2005). Traditionally, composite energetic materials are prepared by mixing physically fine powders of fuel(s) and oxidant(s). Mixing nanoparticles of metal and oxidiser by conventional means can be an extreme fire hazard.

Valliappan *et al.* (2005) developed a method in which very fine particle components of composite energetic material are dispersed into an organic solvent. At a very small size such as nano-size, particle interactions become significantly more influential and, as a result, nanoparticles have a higher tendency to agglomerate (Eisenreich *et al.*, 2005).

The powder mixtures (Figure 3.1) were therefore dispersed in sufficient cyclohexane to make a thick paste. Particle agglomerates were broken down and mixing was effected by grinding in a glass mortar and pestle. Afterwards the organic solvent used was allowed to evaporate at ambient conditions, followed by a final drying step in an oven set at 60 °C.

3.4 Instruments

3.4.1 Thermal conductivity

The ease of ignition of a specific composition is determined by a short time to ignition. For mixtures with high thermal conductivity, the heat dissipates rapidly and consequently a composition becomes less sensitive or difficult to initiate. The key to determining how resistant a material is to conducting heat lies in its composition, microstructure and porosity. A high thermal conductivity for a powder is associated with zero porosity or the presence of metallic components, so most insulators are highly porous (non-metallic), while most heat sinks are dense (German, 2005). Therefore to investigate the combustion reactions in pyrotechnic compositions, values of the thermal conductivity of the powdered material are required (Beck *et al.*, 1984).

As the thermal conductivities of powders are very sensitive to interparticle contact and the pore space, Goldsmid *et al.* (1981) constructed an apparatus that compacts samples and measures their thermal conductivity coefficients, as shown in Figure 3.2.

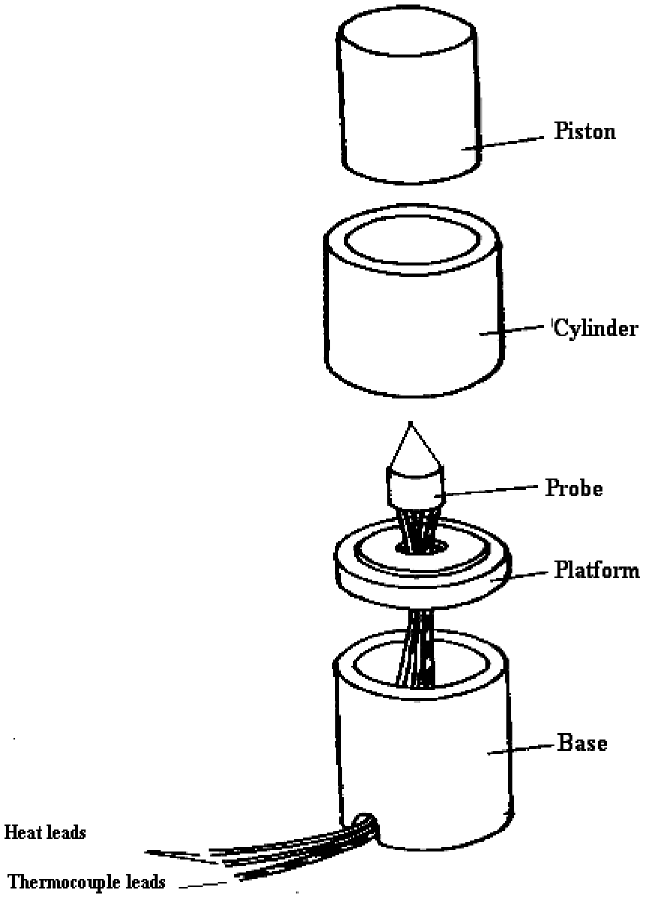

Figure 3.2: Apparatus for compaction of powdered samples (Beck *et al.*, 1984)

In Figure 3.3, the copper probe has a mass of 4.63 g with shape and dimensions are shown. The probe is suitably drilled to allow fitting of an 11 Ω heating resistor connected to a regulated low-voltage DC source. The probe is placed on a recessed Perspex platform and the powder is introduced at the top of the cylinder. A thermocouple, which is fixed to the probe, is used to monitor the temperature of the probe as a function of time.

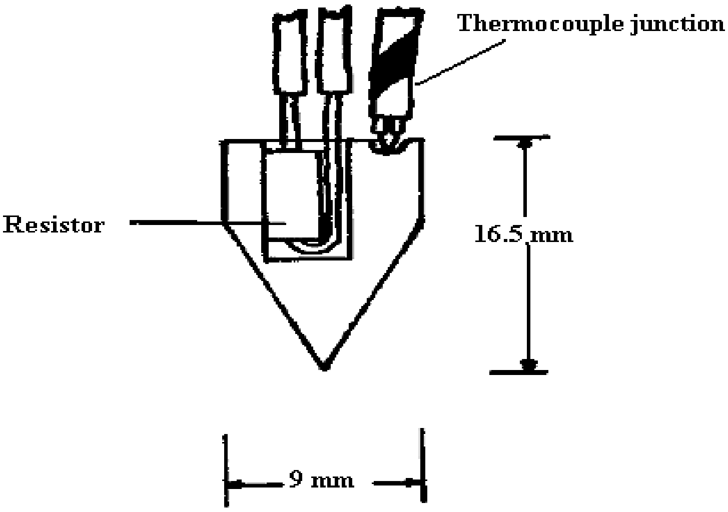

Figure 3.3: Thermal conductivity probe (Beck *et al.*, 1984)

3.4.2 Differential thermal analyser (DTA)

Figure 3.4: High temperature heat-flux DTA-50 SHIMADZU

Knowledge of the thermal behaviour, the stability and the compatibility of pyrotechnic compositions is very important for initiation point determination and therefore for safety.

The apparatus (Figure 3.4) is composed of two identical cells in which the sample and reference are respectively placed. Both cells are heated with a constant heat flux using a single heater and the temperatures of the two cells are measured as a function of time. Alumina sample pans were employed and 5 mg of α-Al_2O_3 was used as reference compound. Two thin copper discs (500 µm thick) were placed at the bottom of the pans. These served to protect the measuring head against the extreme temperature excursions generated by the thermite reactions. Without these discs, severe damage would invariably occur.

3.4.3 Delay time testing pot

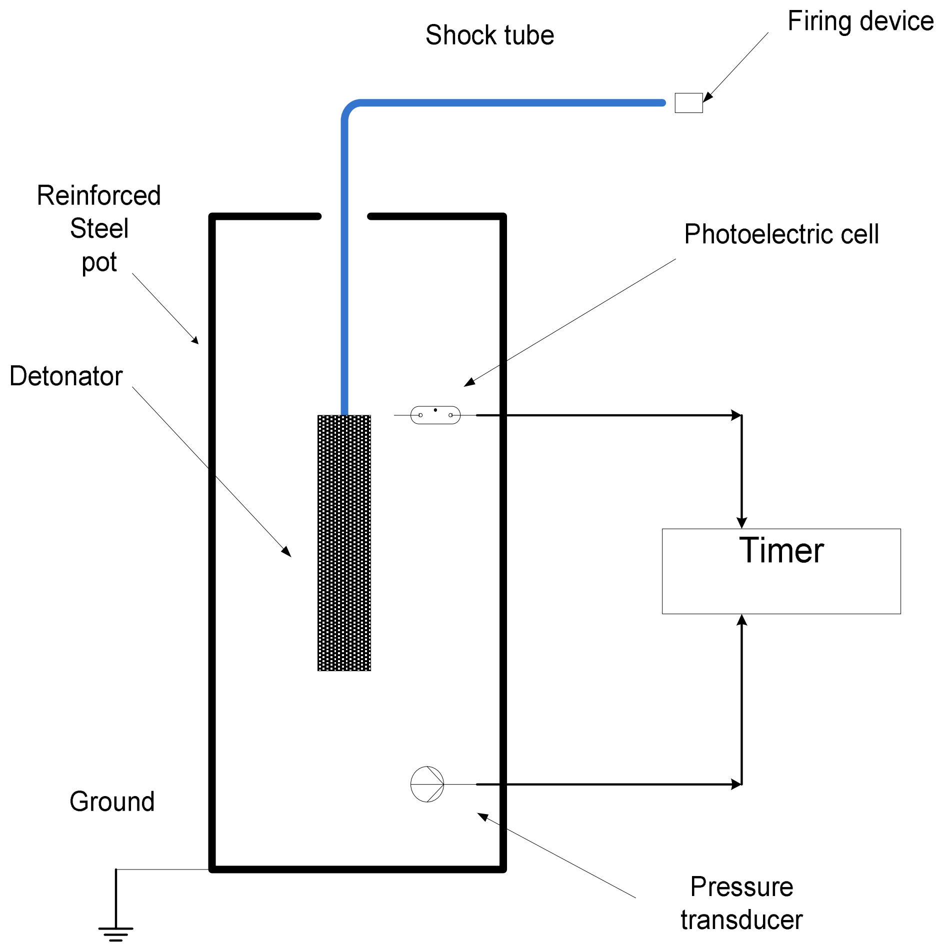

Figure 3.5: Firing and timer circuits

The set-up for measuring the burning time of different compositions may be represented as in Figure 3.5. The unit prepared as described above is assembled as a shock tube detonator, using lead azide as the primary explosive. When the shock tube is ignited by a firing device, the light from the shock tube falls on a photoelectric cell which sends a signal to start the timer. After detonation, a pressure transducer sends another signal to stop the timer. At least five measurements for each composition must be performed, and the mean value is calculated.

3.5 Experimental Methods

3.5.1 Thermal conductivity

The pyrotechnic composition powders used in the apparatus above were sieved to particle sizes < 90 µm. The copper probe was placed on a recessed Perspex platform and the powder poured into the top of the cylinder. Then the piston was introduced and a pressure of 130 kg was applied to compact the sample.

The copper probe was powered by a regulated DC power supply. The input power ($Q = i^2R$) was found from measurements of current and voltage. The current measurements (in amps) across the heating element (11 Ω) were monitored continuously with a precision multimeter. A power of 0.44 W was required to produce a steady-state temperature of the order of 8 °C above ambient temperature. The output from the thermocouple was fed at intervals of 9 seconds to a computer. The data acquisition system recorded the probe temperature for approximately 800 seconds. Thereafter the temperature–time data were plotted.

Aluminium oxide monochromatic powder (α-Al_2O_3) with particle sizes < 90 µm was the standard calibration material. The published value of the measured thermal conductivity of α-Al_2O_3 powder is 0.22 $Wm^{-1}K^{-1}$ (Beck *et al.*, 1984) and the thermal conductivity of the fully densified material is 30 $Wm^{-1}K^{-1}$.

3.5.2 Thermal behaviour

The measuring pan was filled with 5 mg of thermite composition. The powder was pushed down firmly, by hand using a flat punch, against the alumina crucible base.

All experiments were performed in a nitrogen atmosphere to eliminate aerial oxidation of the fuel. The temperature was scanned from ambient to 1 000 °C at a scan rate of 50 °C/min. During the heating process, samples underwent thermal transitions and the DTA captured the difference in temperature.

3.5.3 Burn rate

Safety measures

Superthermites have been found difficult to process safely. The main difficulty is handling of dry nano-size powder mixtures due to the sensitivity to friction and electrostatic discharge of nano-size aluminium or silicon fuels. Thus for safety reasons, nano-size particles are sacrificed to some extent and larger particle sizes are used to minimise accidental ignition by static discharge.

Pressing of compositions in delay elements

A manually operated hydraulic press was used to consolidate the experimental compositions in 23 mm-long aluminium Charlize rigid elements (developed by African Explosives Limited – AEL). Granules of each composition were introduced to the delay element in four equal increments. For all compositions, one increment of G-composition (starter and sealer) was pressed in at the diaphragm side of the Charlize element. Each increment was pressed at 130 kg for a dwell time of 2 seconds. Then each unit was ready for use in the measurement of burning time described above.

CHAPTER 4 RESULTS AND DISCUSSION

4.1 Thermal conductivity

Using the procedure outlined above and for the sake of repeatability and reproducibility of the output from the thermocouple, five measurements were conducted with the above-described probe using chromatographic alumina as reference material. The temperature–time curves obtained from these were very close one to another.

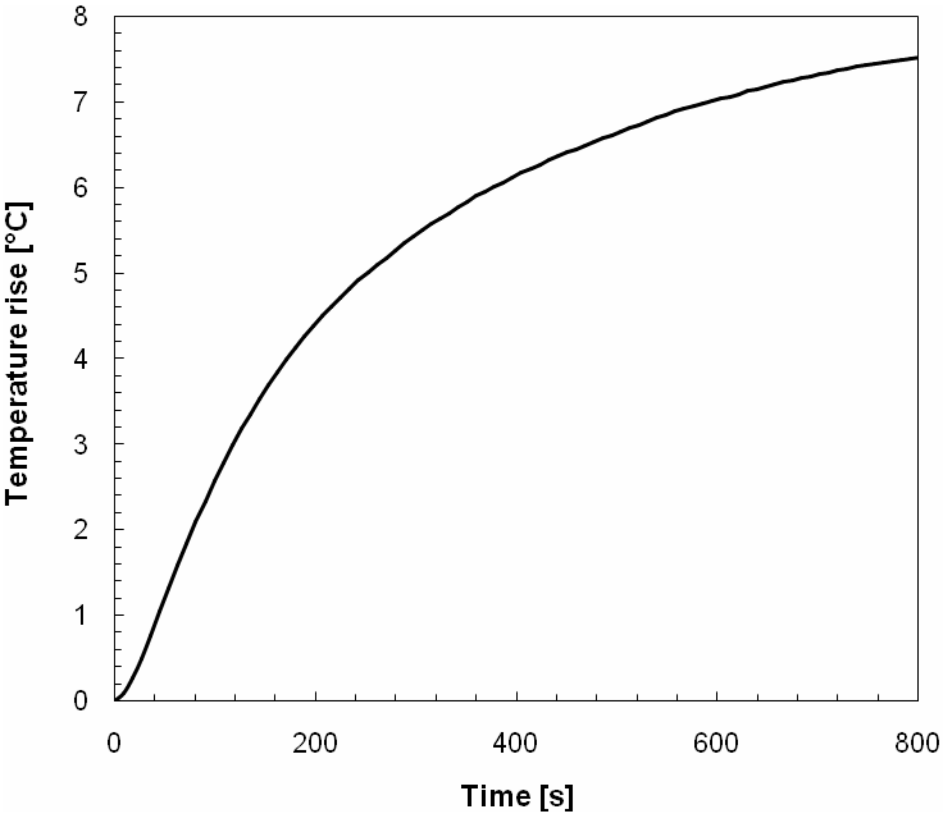

Figure 4.1: Temperature–time curve of α-Al_2O_3 powder

The average temperature–time curve of the five measurements was plotted and is shown in Figure 4.1. The variation in experimental data for the temperature–time curve of α-Al_2O_3 powder was quantified by calculating the standard deviation (SD). This latter statistical value is approximately the average of the difference between each value and the mean. It is also a measurement of variation in experimental data due to errors caused by equipment, personnel, sample homogeneity and other uncontrollable factors (e.g. room temperature). In other words, it indicates how well the whole experiment was carried out.

According to the temperature–time data obtained, the average value of SD was found to be 0.16. This relatively small SD indicates that the thermal probe method gives repeatable and reproducible measurements of the temperature–time data.

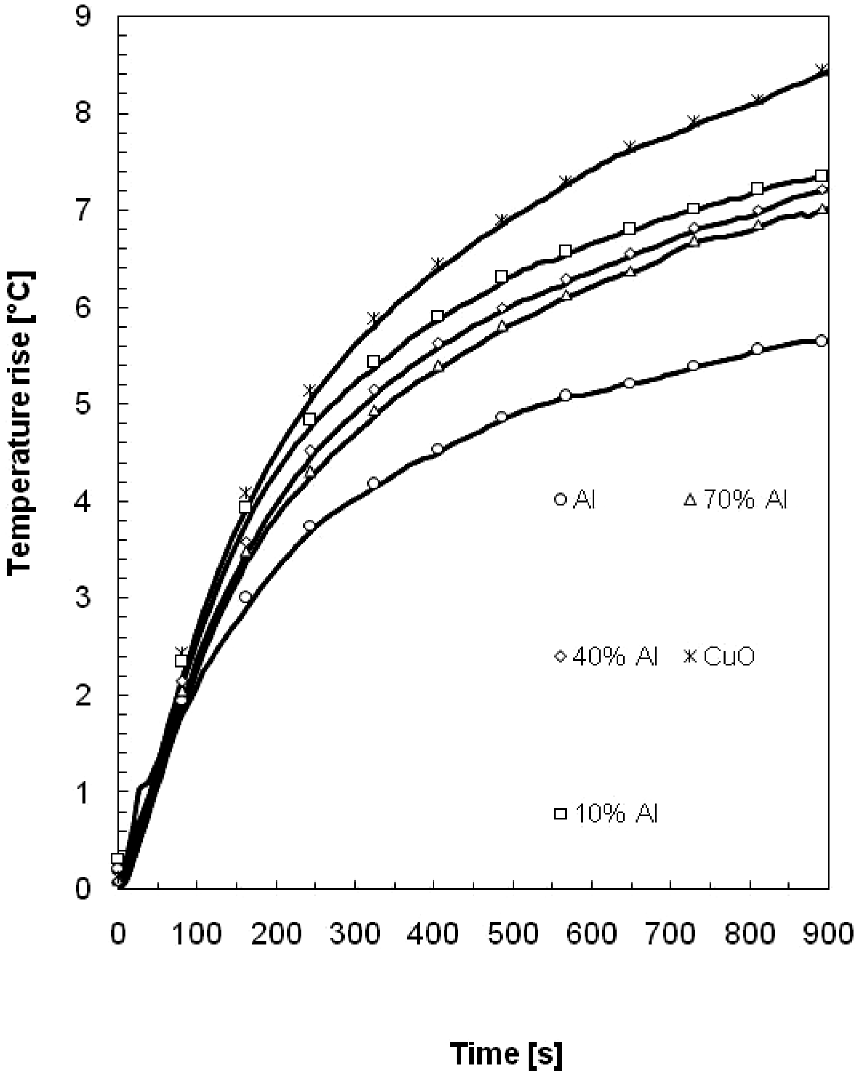

Figure 4.2: Temperature–time curves with different Al contents

Temperature–time curves of the Al-CuO thermite system with different oxygen balances (10, 40 and 70% Al) are shown in Figure 4.2. All curves are ascending. According to the equation of Carslaw and Jaeger (Beck *et al.*, 1984), the temperature rise of the powder is inversely proportional to the thermal conductivity.

Therefore, the lowest curve corresponds to the composition with the highest thermal conductivity coefficient.

Therefore, the higher the amount of aluminium in the mixture, the higher the thermal conductivity coefficient. This may be explained by the fact that in the Al-CuO thermite system, it is mostly the free electrons from the aluminium particles that transfer heat energy. These electrons are free to move easily through the mixture. Therefore the thermal energy is picked up by the free electrons and rapidly transferred from one particle to another at the point of contact.

The temperature–time curves of the mixture of 19%Al-81%CuO and different percentages of the 20% Si-80% Bi_2O_3 system are shown in Figure 4.3.

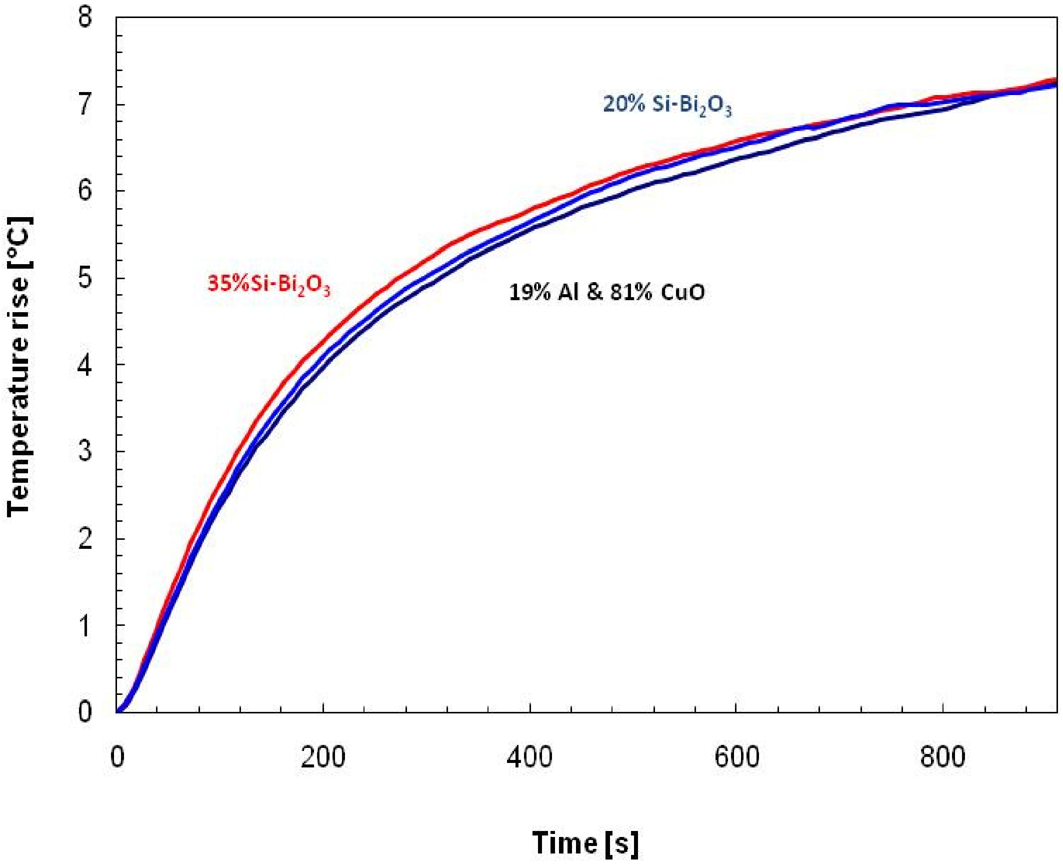

Figure 4.3: Temperature–time curves for Al-CuO system and Si-Bi_2O_3 additive

The addition of 20 and 35% of the Si-Bi_2O_3 system does not influence significantly the thermal conductivity of the 19%Al-81%CuO thermite composition. The thermite mixtures still have the same thermal conductivity as the Al-CuO thermite system.

4.2 Thermal behaviour of Al-CuO thermite and Al-CuO/Si-Bi_2O_3 mixture

Figure 4.4 shows the DTA response for a stoichiometric Al and CuO mixture comprising coarse aluminium and nano-sized CuO particles.

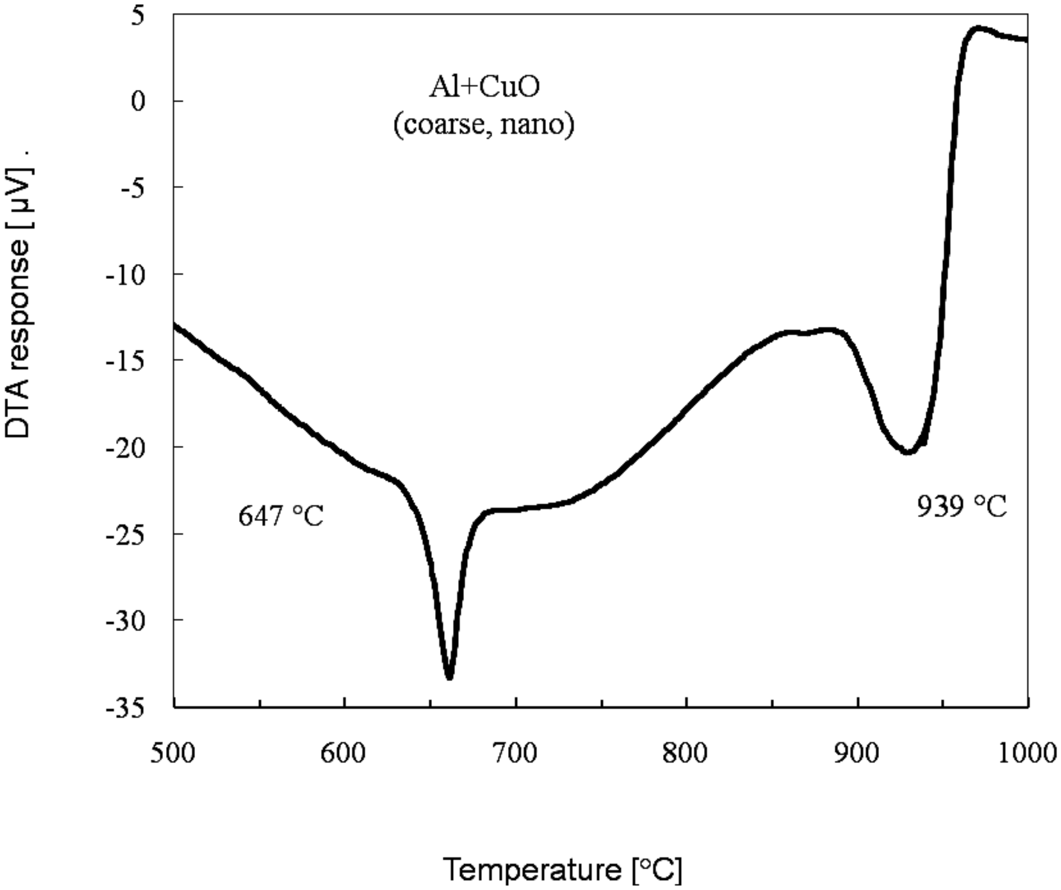

Figure 4.4: DTA response of stoichiometric Al-CuO compositions comprising coarse aluminium and nano-sized CuO particles

The first endotherm has an onset temperature of 647 °C and corresponds to the melting point of aluminium metal. The second endotherm, which has an onset temperature at 939 °C, probably corresponds to the melting and dissolution of CuO in the aluminium melt. This is followed by a fast exotherm with an onset temperature of ca. 939 °C. This exotherm is identified with the ignition temperature of the composition leading to oxidation of the aluminium. When CuO is replaced by a stoichiometric amount of Bi_2O_3, the ignition temperature is lowered to ca. 801 °C. This thermal behaviour suggests that the mechanism of reaction for Al-CuO is based on liquid-liquid diffusion.

Consequently, the time to ignition will obviously be longer since both constituents require a phase change before the reaction takes place. This might be one of the reasons why micron-size thermite incendiary devices are difficult to ignite. Therefore a pyrotechnic system that reacts between the two melting temperatures of the thermite system can be used as a 'burn catalyst' to reduce sensibly the ignition delay time and the ignition temperature of the Al-CuO thermite system.

The thermal behaviour of the Si-Bi_2O_3 system (Figure 4.5) shows a small endotherm in the temperature range of 729–735 ℃, which corresponds to the α-Bi_2O_3 phase transformation to the δ-Bi_2O_3 phase (the literature states that the temperature should be above 727 °C).

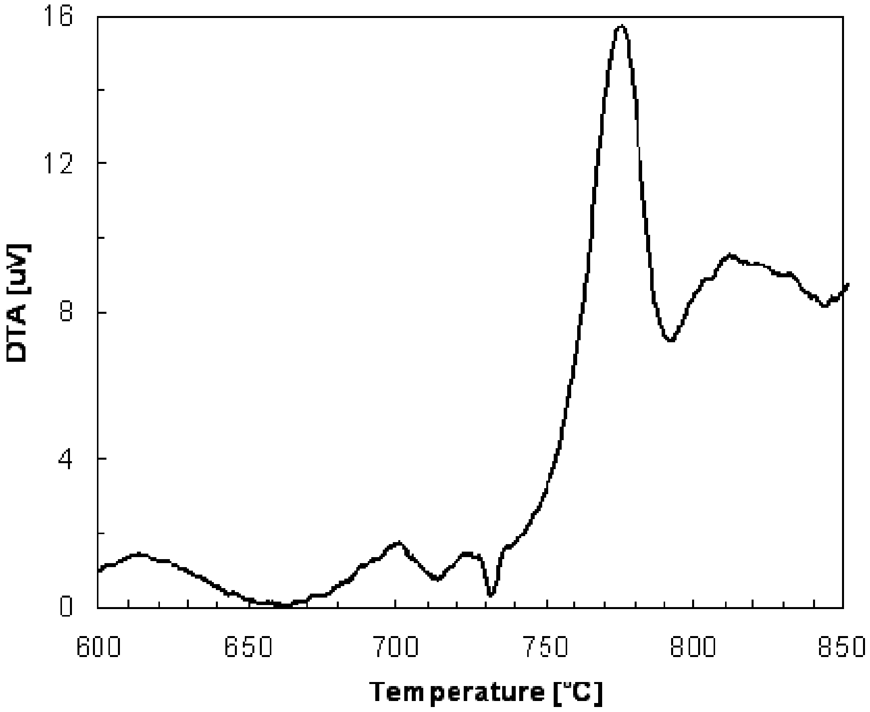

Figure 4.5: Thermal behaviour of the Si-Bi_2O_3 system reaction

In the temperature range of 758–788 °C an exothermal process occurs which can be attributed to the reaction between silicon and the oxygen ions released by the δ-Bi_2O_3 phase. The δ-Bi_2O_3 phase has a defective fluorite-type crystal structure in which two of the eight oxygen sites in the unit cell are vacant. The intrinsic vacancies are highly mobile due to the high polarisability of the cation sublattice with the $6s^2$ lone pair of electrons of Bi^{3+}. The Bi-O bonds have a covalent bond character and are therefore weaker than purely ionic bonds, so oxygen ions can jump into the vacancies more freely (Sammes *et al.*, 1999).

Figure 4.6 and the explanation above suggest the hypothesis that the mechanism for the Si-Bi_2O_3 reaction is based on solid-solid diffusion, and then the heat released by the Si-Bi_2O_3 reaction triggers the Al-CuO thermite reaction by lowering the melting temperature of CuO.

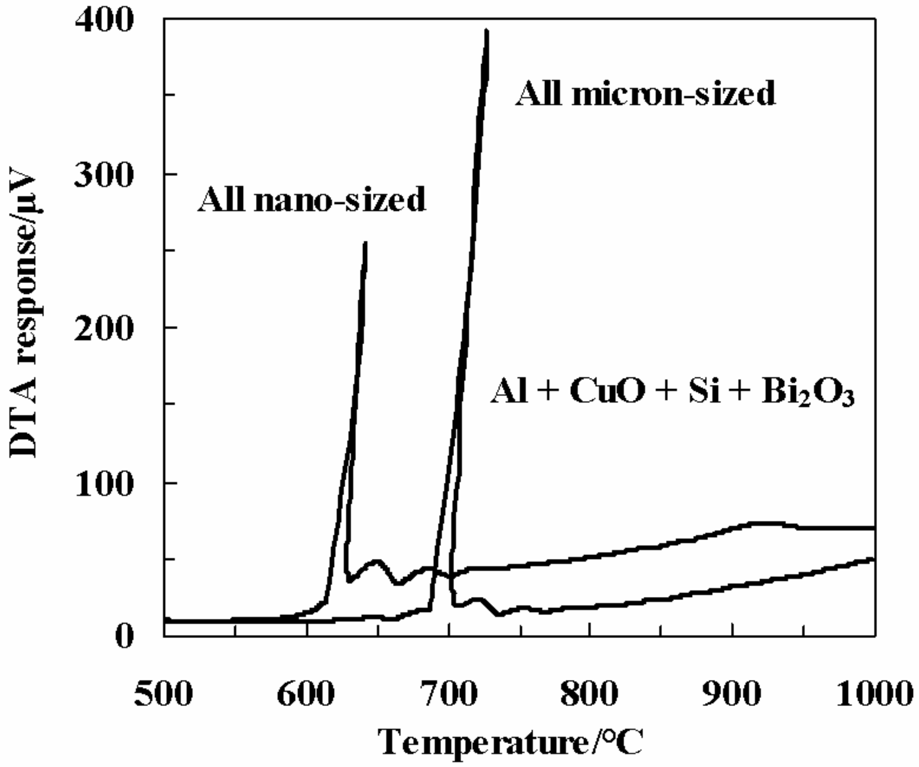

Figure 4.6: Thermal behaviour of Al+CuO+Si+Bi_2O_3 made up with coarse particles

Figure 4.6 shows the DTA response of a mixture containing 80 wt % thermite (Al-CuO) and 20 wt % sensitiser (Si-Bi_2O_3), all components nano-sized or micron-sized. The DTA response features much stronger and sharper exotherm peaks (corresponding to thermal runway situations) than the one shown in Figure 4.6. The onset temperature is 689 °C for the system comprising micron-sized powders. The ignition temperature is lowered to 613 ^{o}C if only nano-sized powders are used. In both cases the exotherms show an extreme temperature rise that far exceeds that observed for the thermite itself. The thermal runway is so fast that it approaches a 'thermal explosion'. This is substantiated by the fact that in both cases the alumina sample pans were shattered.

4.3 Ignition temperature

The ignition temperature is an important thermal property required to ensure combustion process operations. An alternative initiator is attractive when it is easily initiated by the application of a specific stimulus (e.g. heat) to a small portion of its mass.

4.3.1 Effect of particle size, sensitiser content and stoichiometry on the onset ignition temperature

The effect of particle size on the ignition temperature is summarised in Table 4.1.

Table 4.1: Ignition temperatures of mixtures (compositions indicated in wt % and size given)

Thermite		**Sensitiser (tinder)**		**Onset/ignition temperature [°C]**
81.7	**18.3**	**80**	**20**	
CuO	**Al**	**Bi_2O_3**	**Si**	
micron	micron	-	-	942
nano	micron	-	-	939
nano	nano	-	-	942
-	-	micron	micron	935
-	-	nano	nano	747

Thermite		**Sensitiser (tinder)**		**Onset/ignition temperature [°C]**
65.3	**14.7**	**16**	**4**	
CuO	**Al**	**Bi_2O_3**	**Si**	
micron	micron	micron	micron	689
nano	nano	micron	micron	737* and 733*
micron	micron	nano	nano	No exotherm
nano	micron	nano	nano	727
nano	nano	nano	nano	613* and 610*

* Thermal runaway

The ignition temperature of the Al-CuO thermite is about 940 °C irrespective of the particle size of the reactants. The ignition temperature of the Si-Bi_2O_3 pyrotechnic mixture is affected by particle size. The ignition temperature is 935 °C for a coarse powder mixture. This drops down to about 747 °C when the mixture is composed of nano-sized powders.

Thermal runaway was observed for the sensitiser ('burn catalyst') mixtures when the component powders of the thermite were both nano-sized, but this also applied to all the powders used. The ignition temperature for the all-nano mixtures was significantly lower ($T_i \approx 613$ ºC) than those for the all-coarse mixture ($T_i \approx 689$ °C) and for the all-nano-thermite + all-coarse-sensitiser ($T_i \approx 735$ °C) mixture. No thermal runaway was observed for the other mixtures listed in Table 4.1.

Table 4.2 details the effect of varying the amount of Si-Bi_2O_3 sensitiser ('burn catalyst') on the ignition temperature. Thermal runaway occurs at 20 wt % sensitiser content and the lowest ignition temperature is also attained at 20 wt % sensitiser content ($T_i \approx 613$ °C). The thermite composition was stoichiometric while the Si: Bi_2O_3 ratio was 4:1.

Table 4.2: Effect of sensitiser content on the onset/ignition temperatures (compositions indicated in wt %)

Thermite			Sensitiser (tinder)			Onset/ignition temperature [°C]
Al nano	CuO nano	Total [%]	Si nano	Bi_2O_3 nano	Total [%]	
16.6	73.4	90.0	2.0	8.0	10.0	732
15.9	69.0	84.9	3.0	12.1	15.1	623
14.7	65.3	80.0	4.0	16.0	20.0	613*
14.0	61.1	75.1	5.0	20.0	25.0	620

*Thermal runway

Table 4.3 reports on the effect of varying the stoichiometry of the Al-CuO thermite composition. The results indicate that the lowest ignition temperature is attained at the stoichiometric Al-CuO thermite composition (14.5% Al). Again, this was the only one that led to a thermal runaway.

Table 4.3: Effect of thermite stoichiometry on the onset/ignition temperature (compositions indicated in wt %)

Thermite			Sensitiser (tinder)			Onset/ignition temperature [°C]
Al nano	CuO nano	Total [%]	Si nano	Bi_2O_3 nano	Total [%]	
20.0	60.0	80.0	4.0	16.0	20.0	621
15.9	64.1	80.0	4.0	15.9	19.9	622
14.5	65.6	80.1	4.0	16.0	20.0	610
12.1	68.0	80.1	4.1	15.8	19.9	621

Nano-sized thermite plus tinder compositions feature a much lower ignition temperature than micrometre-sized compositions. The thermite mixture with 20% Si-Bi_2O_3 system and 80% Al-CuO thermite system (stoichiometric) exhibits the lowest ignition temperature. Therefore, the thermite composition with the lowest ignition temperature and giving an explosive reaction is determined as follows: 65% CuO, 15% Al, 4% Si and 16% Bi_2O_3.

Table 4.4 presents the effect of other compositions on the ignition temperature when all components are nano-sized. The ignition temperature of the stoichiometric mixture of aluminium and bismuth trioxide is quite high as well (i.e. 801 ºC). The onset temperatures for the other compositions listed in Table 4.4 show that just adding small amounts of either silicon or bismuth trioxide to the thermite only leads to a reduction in the ignition temperature. It is worth noting that adding a substantial quantity of bismuth trioxide did lead to thermal runaway.

Table 4.4: Effect of other compositions on the onset/ignition temperature (compositions indicated in wt %)

Thermite			Sensitiser (tinder)			Onset/ignition temperature [°C]
Al nano	CuO nano	Total [%]	Si nano	Bi_2O_3 nano	Total [%]	
17.7	78.3	96.0	4.0	-	4.0	895
17.0	75.0	92.0	8.0	-	8.0	884
15.5	68.3	83.8	-	16.2	16.2	789
14.7	64.7	79.4	-	20.6	20.6	806
11.7	12.8	24.5	-	75.5	75.5	734*
10.4	-	10.4	-	89.6	89.6	801
6.8	-	6.8	14.2	79.0	93.2	No exotherm

*Thermal runway

The melting temperatures of the aluminium powders determined by differential scanning calorimetry (DSC) were ca. 598 °C and 654 °C for the nano-sized and micron-sized powders respectively. Interestingly, in each case the observed ignition temperatures were slightly higher than the corresponding melting point of the aluminium powder used as fuel. This suggests the following hypothesis for explaining the observed thermal runaway results. The presence of copper oxide acts as a catalyst; the reaction of the silicon with bismuth oxide is facilitated by the aluminium turning into a liquid. The concomitant energy release provides the required activation energy required to 'kick-start' the thermite reaction between the aluminium and the copper oxide, allowing it to proceed at an extremely fast rate.

4.4 Burn rate

Figure 4.7 reports burn rates for the Al-CuO thermite sensitised by 25 wt % Si-Bi_2O_3 using only micro-sized powders. The average maximum burn rate of 313 mm/s was achieved at an aluminium content of 14.2% in the mixture. The observation that the burn rate of the quaternary mixture, comprising micron-sized powders, exceeds that of the fast-burning Si-Bi_2O_3 system is highly significant.

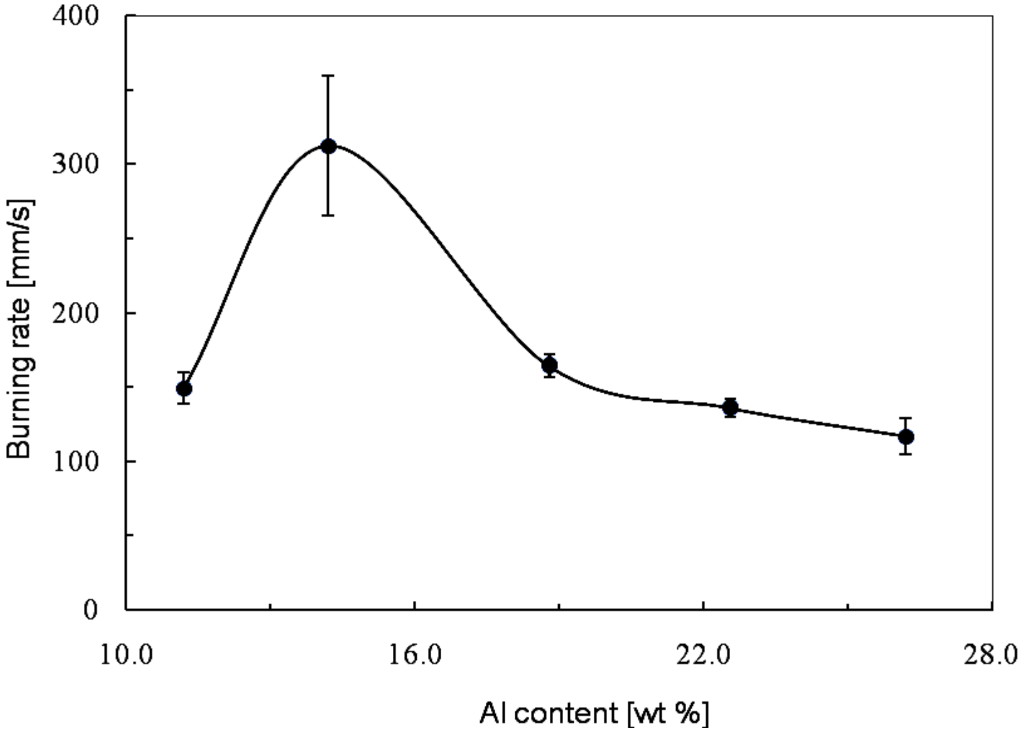

Figure 4.7: Burn rate of Al+CuO+Si+Bi_2O_3 with different Al contents pressed in Charlize element at 130 kg

Consolidated compositions with a large excess of Al, above 28%, did not ignite. An X-ray image of a misfire sample is shown in Figure 4.8. For reactions where a large excess of Al is present, the solid-solid mechanism prevails; the surface area of Al and good fuel/oxidiser contact are the controlling factors. With a large excess of Al, the reactions are incomplete owing to some Al particles not being in contact with the oxides (poor oxygen balance). Furthermore, an excess of Al (unreacted) will act as a heat sink as it melts and keep the temperature constant until the entire Al content is molten. Therefore, the presence of misfires may be associated with the high thermal conductivity and low oxygen balance achieved by these compositions, which increase tremendously the time to ignition. On the X-ray image, it can be noticed that the interface between the starter composition (G-composition) and the first increment of the Al-CuO thermite mixture started to burn but failed to propagate ($E_f < E_a$).

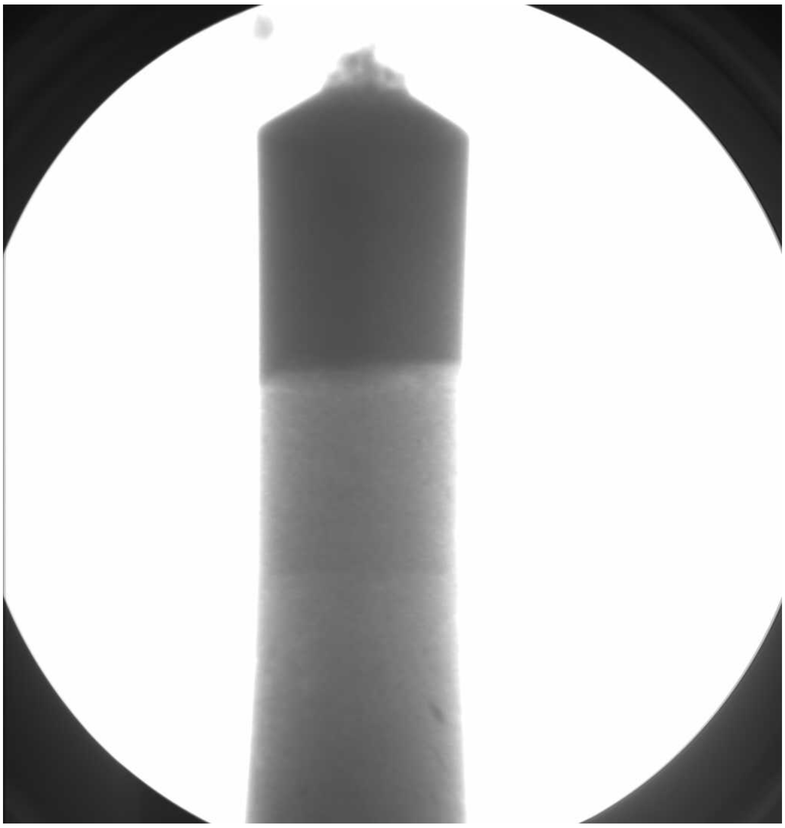

Figure 4.8: X-ray image of a misfire sample with 28% Al wt content

For the stoichiometric mixture of micro-sized Al-CuO thermite composition sensitised with 20 wt % Si-Bi_2O_3 pyrotechnic mixture, visual observation during the burn test of powders pressed in aluminium Charlize elements indicated that the reaction is violent. The high pressures inside the aluminium rigid elements led to bursting. Figure 4.9 shows one of the four samples of detonators destroyed on top of the Charlize element after the shock tube had been fired. The rate of reaction of this composition is very dependent on the pressures formed. Reactions will depend on the diffusion of vaporised oxides into the surface Al and products. It is speculated that the acceleration of the vaporised oxides depends on the direction of the gas transport, either forwards or backwards, depending on the location of leaks. That may explain the damage done at the diaphragm of the Charlize element.

Figure 4.9: Destroyed detonator with aluminium Charlize element filled with thermite composition containing 20 wt % sensitiser

However, replacing the aluminium rigid elements with custom-made steel tubes solved this problem. The burn rate of the thermite with 14.5% Al (14.5% Al; 65.5% CuO; 4% Si (type 4); 16% Bi_2O_3), using a steel Charlize rigid element, was 655 ± 67 mm/s. Table 4.5 gives more details on the measurement of the burn rate of the 14.5% Al composition filled in a steel element.

The burn rate of the 14.5 wt % Al (80% Al-CuO and 20% Si-Bi_2O_3) thermite composition pressed in a steel Charlize rigid element is twice as fast as the burn rate of aluminium Charlize rigid elements filled with 14.2 wt % Al (75% Al-CuO and 25 % Si-Bi_2O_3).

Table 4.5: Burn rate of 14.5 % Al composition filled in steel element

Trial	Stack height (mm)	Real stack height (mm)	Timing (ms)	Burn rate (mm/s)
1	24.47	23.1	39.1	589.8
2	23.70	22.3	38.4	580.5
3	23.69	22.3	36.6	608.7
4	23.65	22.2	36.3	612.7
5	23.60	22.2	36.2	613.0
6	23.58	22.2	35.8	619.3
7	24.47	23.1	31.2	739.1
8	23.43	22.0	30.8	714.9
9	23.37	22.0	29.9	734.4
10	23.30	21.9	29.6	739.5
Min	23.30	21.9	29.6	580.5
Max	24.47	23.1	39.1	739.5
Mean	23.73	22.3	34.4	655.2
SD	0.41	0.4	3.6	67.4

Real stack height = Stack height – Diaphragm (1.41 mm)

CHAPTER 5 CONCLUSIONS AND RECOMMENDATIONS

The aim of this research was to explore further sensitisation of the Al-CuO thermite system by the fast-burning Si + Bi_2O_3 pyrotechnic composition (mass ratio 1:4) used as tinder, for both micron-sized and nano-sized thermite mixtures, using differential thermal analysis (DTA). The effects of particle size (micron vs. nano), thermite stoichiometry and the amount of sensitiser were investigated.

Thermal runaway was observed only for the stoichiometric 2Al + 3CuO thermite composition in the presence of sufficient sensitiser. The lowest ignition temperatures were obtained with stoichiometric thermite mixtures containing 20 wt % sensitiser. The ignition temperature was 613 °C when the mixture comprised nano-sized powders. When coarse, micron-sized powders were used instead, the ignition temperature was 689 °C. In both cases the ignition event led to a thermal runaway reaction, creating a temperature shock severe enough to cause the disintegration of alumina sample pans. Instead, no thermal runaway is found at a slightly higher sensitiser content of 25 wt %. The Al-CuO thermite system containing 20 wt %, comprising micron-sized powders, may provide a fast-burning replacement alternative for the red lead-silicon system used in millisecond time delays. The lead-based system needs to be replaced owing to environmental concerns and the thermite system presents a 'greener' option.

Compositions containing more than 28 wt % Al did not ignite. The misfires may be associated with the high thermal conductivity and low oxygen balance achieved by these compositions, which increase tremendously the time to ignition.

Therefore the Al-CuO fast-burning replacement alternative for the toxic Si-Pb_3O_4 pyrotechnic composition, with all components micro-sized, is as follows: 65.5 wt % CuO, 14.5 wt % Al, 16 wt % Bi_2O_3 and 4 wt % Si.

CHAPTER 6 REFERENCES

Aumann C.E., Skofronick G.L., Martin J.A. (1995) Oxidation behaviour of aluminium nanopowders. *J. Vac. Sci. Technol., B: Microelectron. Nanometer Struct. Process, Meas., Phenom.,* 13, 1178–1183.

Beck, M.W, Brown, M.E. and Heideman, N.J.H. (1984) Application of a probe technique for measuring the thermal conductivity of pyrotechnic compositions. *J. Phys. E: Sci. Instrument.*, 17, 794-799.

Berger, B. (2005) Parameters influencing the pyrotechnic reaction. *Propellants, Explosives, Pyrotechnics* 30(1), 27-35.

Bockmon, B.S., Pantoya, M.L., Son, S.F., Asay, B.W., Mang, J.T. (2005) Combustion velocities and propagation mechanisms of metastable interstitial composites. *J. Appl. Phys.,* 98 (064903), 1–7.

Booth, F. (1958) The theory of self-propagating exothermic reactions in solid systems. *Trans. Farad. Soc.,* 49, 272–281.

Carslaw, H.S., Jaeger, J.C. (1975) *Conductivity of Heat in Solids*, 2nd ed. Oxford: Clarendon.

Charley, E.L., Laye, P.G. and Brown, M.E. (2001) *Hand book of thermal analysis and calorimetry. Vol 2: Applications to inorganic and miscellaneous materials*. Brown, M.E and Gallagher, P.K editors.

Conkling, J. A. (1985) *Chemistry of Pyrotechnics: Basic Principles and Theory*. Publisher: M Dekker. United States.

Conkling, J. (1990) Pyrotechnics. *Scientific American*, July 1990, 108.

Crider, J.F. (1982) Self-propagating high-temperature synthesis. A Soviet method for producing ceramic material, 519-526.

Edward, L.D. (2009) Metal-based reactive nanomaterials. Progress in Energy and combustion science 35, 141-167

Erickson, J., Andover, M.M., Sandstrom, J.L., Corcoran, M.N., Johnston, G (2008) Non-toxic percussion primers and methods of preparing the same. Patent Application Publication. US 2008/0245252 A1.

Fisher, S.H. Grubelish, M.C. (1998) Theoretical energy release of thermites, intermetallics and combustible metals. Presented at the 24th International Pyrothenics Seminar, Monterey, CA, US.

Gash, E.A., Tillotson, T.M., Satcher,J.H., Poco, J.F., Hrubesh, L.W., Simpson, R.L. (2001) Use of epoxides in sol-gel synthesis of porous Iron(III) oxide monoliths from Fe(III) salts. Chem.Mater., vol 13, n03, 999-1007.

German, R.M, Ham, V. (1979) Observations on the compaction of binary thermite powder mixtures, Powder Technol. 22, 283–285.

German, R.M. (2005) *A–Z of Powder Metallurgy*, 1st ed. Oxford: Elsevier, Advanced Technology.

Goldsmid, H.J, Davies, K.E. Papazian, V. (1981) Probes for measuring the thermal conductivity of granular materials. *J. Phys. E: Sci. Instrument.,* 14, 1149–1152.

Granier, J.J., Pantoya, M.L. (2004) Laser ignition of nanocomposite thermites. *Combustion and Flame*, 138(4), 373–383.

Guy, A.G. (1976) *Essentials of Materials Science.* New York: McGraw Hill, pp 111–174.

Hannay, N.B. and Bruce, N. (1976) Treatise on solid state chemistry: Volume 4 Reactivity of Solids, Murray Hill, New Jersey

Hunt, E.M., Pantoya, M.L. (2005) Ignition dynamics and activation energies of metallic thermites: From nano- to micron-scale particulate composites. *J. Appl. Phys.*, 98(034909), 1–8.

Kalombo, L., Del Fabbro, O., Conradie C., Focke, W.W. (2007) Sb_6O_{13} and Bi_2O_3 as oxidants for Si in pyrotechnic time-delay compositions. *Propellants, Explosives, Pyrotechechnics,* 32, 454–460.

Khaikin, B.I., Merzhanov, A.G. (1966) Theory of thermal propagation of a chemical reaction front. *Comb. Exp. Shock Waves*, 2, 36.

Kosanke, K.L., Kosanke, B.J., Sturman, B., Shimizu, T., Wilson, M.A., Maltitz, I.V., Hancox, R.J., Kubota, N., Jennings-White, C., Chapman, D. (2004), *Pyrotechnic Chemistry*. Journal of Pyrotechnic Inc.

Kubaschewski, O., Alcock, C.B., Spencer, P.J. (1993) Materials Thermo-Chemistry, 6th edition. New York: Pergamon Press.

McLain, J.H. (1980). *Pyrotechnics from the Viewpoint of Solid-State Chemistry.*, Philadelphia: Franklin Institute Press.

Munir, Z.A. (1988). Synthesis of high-temperature materials by self-propagating combustion methods. *Ceramics Bulletin*, 67(2), 342–349.

Oxtoby, D.W. and Nachtrieb, N.H. (1986) Principles of modern chemistry, Saunders College Publishing CBS Publishing Japan Ltd.

Prakash, A., McCormick, A.V., and Zachariah, M.R. (2004). Aero-Sol-Gel Synthesis of Nano-porous Iron-Oxide Particles: A Potential Oxidizer for Nano-energetic Materials” Chem. Mater., 16, 1466-1471.

Puszynski, J.A., Bulian, C.J., Swiatkiewicz, J.J. (2006) The effect of nanopowder attributes on reaction mechanism and ignition sensitivity of nanothermites. *Mater. Res. Soc. Symp. Proc.*, 896, 147–158.

Rugunanan, R.A (1991) Intersolid Pyrotechnic Reactions of Silicon, PhD thesis, Rhodes University, South Africa.

Sammes, N.M., Tompsett, G.A., Cai, Z.H. (1999) Solid *State Ionics,* 21, 1–4.

Schoenitz, M., Edward, L., Dreizin, E.L. (2005) Energetic materials: performance and safety. Proc. 36th International Annual Conference of ICT & 32nd International Pyrotechnics Seminar, Karlsruhe, Germany, pp 133–136.

Shakhashiri, B.Z. (1989) *Chemical Demonstration. A Handbook for Teachers of Chemistry*, Vol.1. Wisconsin.

Shoshin, Y., Mudry, R.S (2002) Preparation and characterization of energetic Al-Mg mechanical alloy powders. *Combustion and Flame,* 128, 259–269.

Stamatis, D., Jiang, Z., Hoffmann, V.K., Schoenitz, M., Dreizin, E.L. (2009) Fully dense, aluminium-rich Al-CuO nanocomposite powders for energetic formulations. *Combust. Sci. Technol.* 181, 97–116.

Steinhauser, G and Klapotke, TM (2008) ““Green” Pyrotechnics: A chemist’s challenge”, Angew.Chem.Int, 47, 3330-3347.

Tillotson, T.M., Gash, A.E., Simpson, R.L. (2001) Nanostructured energetic materials using sol-gel methodologies. *J Non-Crystalline Solids*, 285, 338–345.

Valliappan, S., Swiatkiewicz, J.J., Puszynski, J.A. (2005) Reactivity of aluminium nanopowders with metal oxides. *J Powder Technology* 156, 164–169.

Van Vlack, L.H. (1970) *Materials Science for Engineers.* Reading, Mass, US: Addison-Wesley, pp 296–306.

Wang, L.L., Munir, Z.A., Maximov, Y.M. (1993) Review of thermite reactions: Their utilization in the synthesis and progressing of materials. *J Materials Science*, 28, 3693–3708.

Wilson, M.A., Hancox, R.J. (2001) Pyrotechnic delays and thermal sources. *J Pyrotechnics*, Issue 13, summer, 9–30.

APPENDICES

Figure A: Micron aluminium

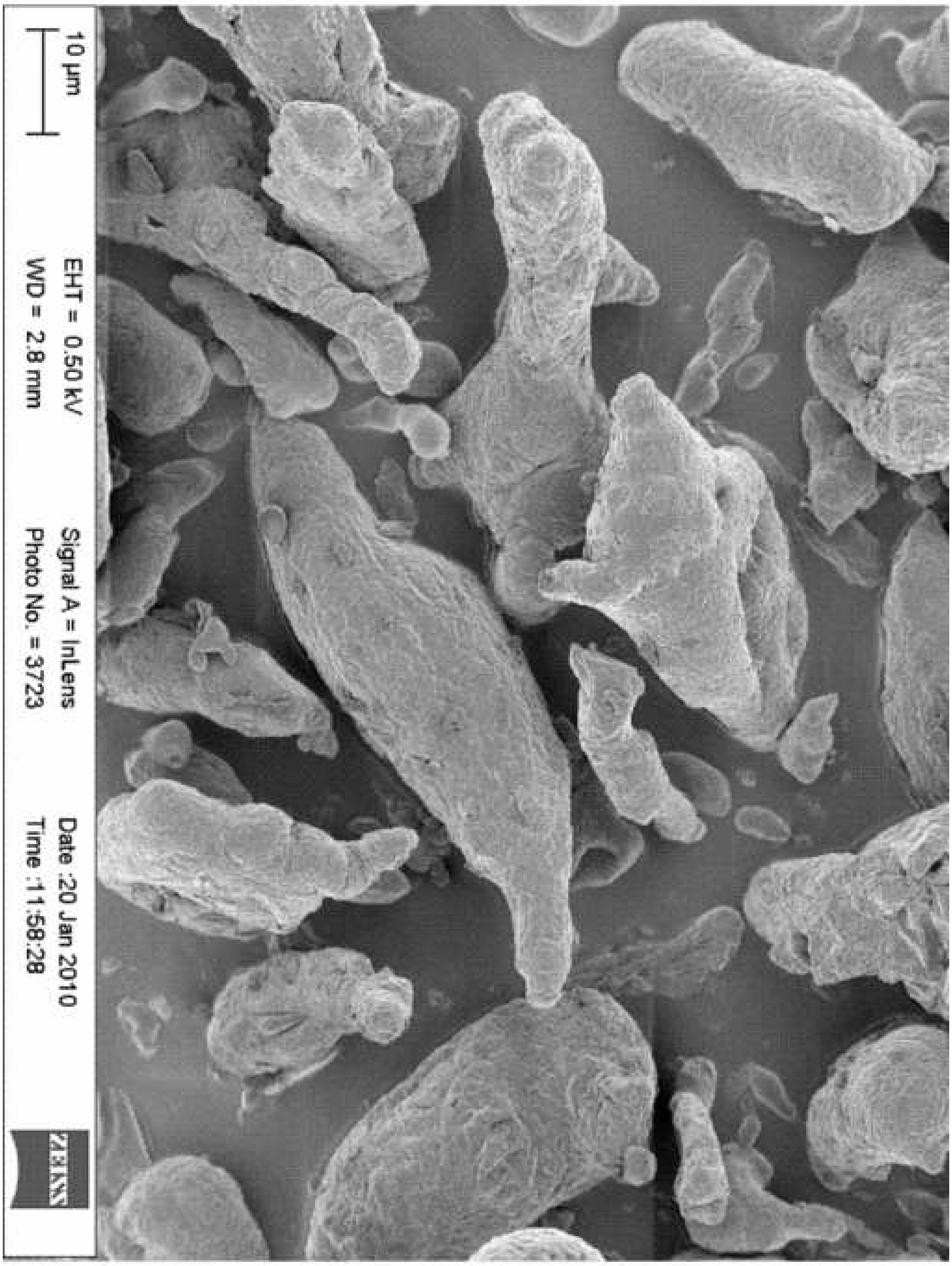

Figure B: Nano-aluminium

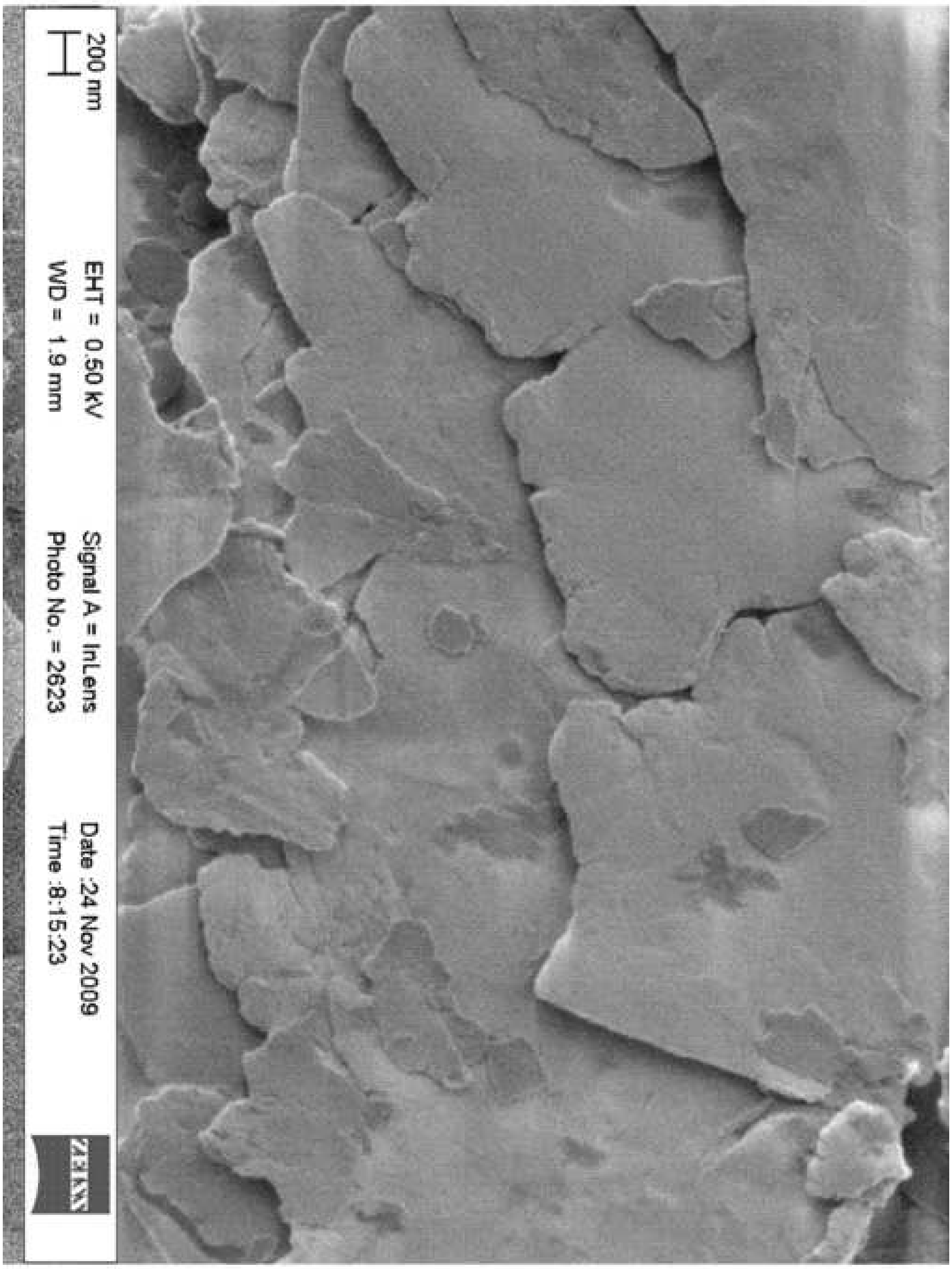

Figure C: Silicon type 4

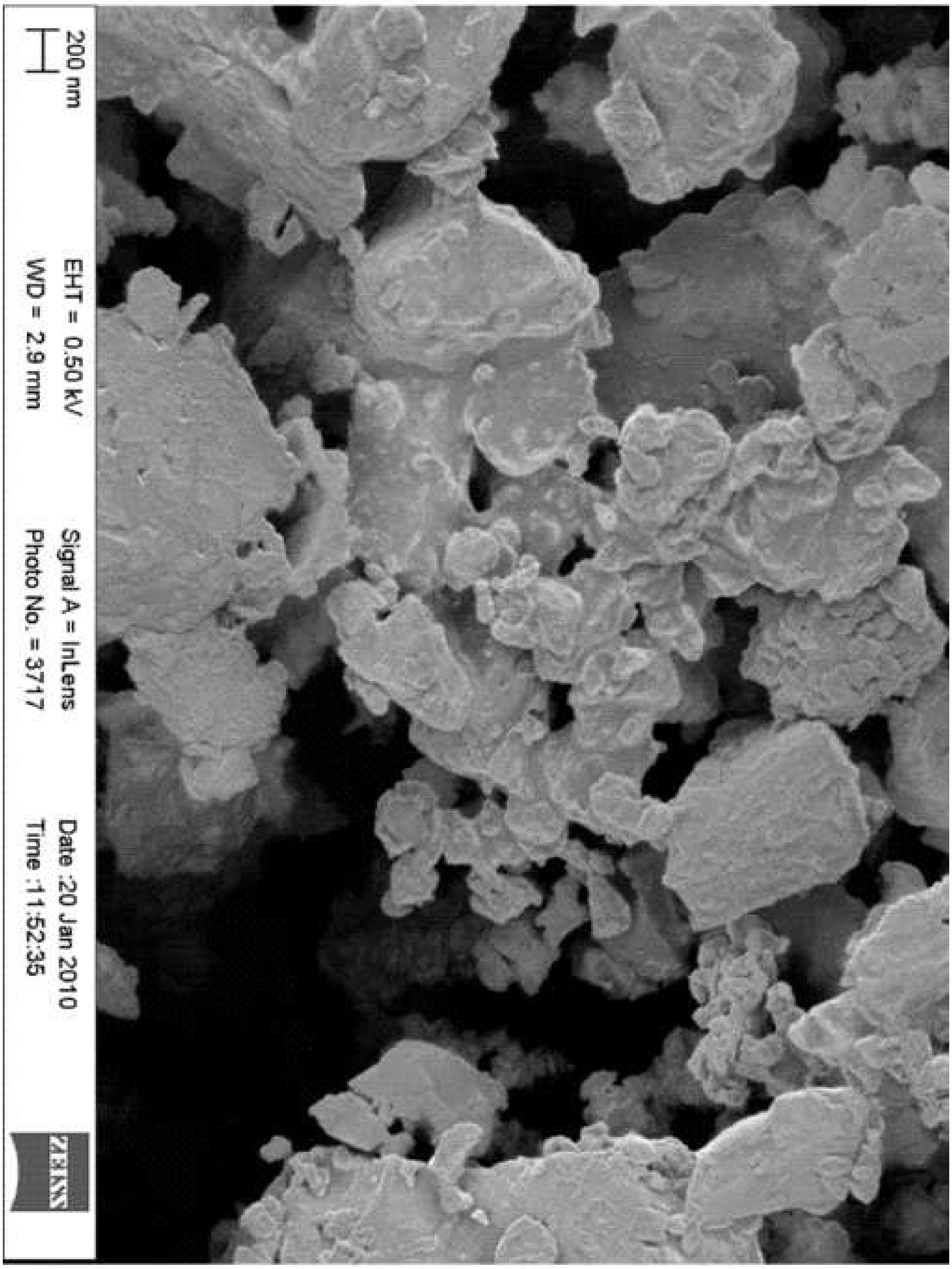

Figure D: Nano-silicone

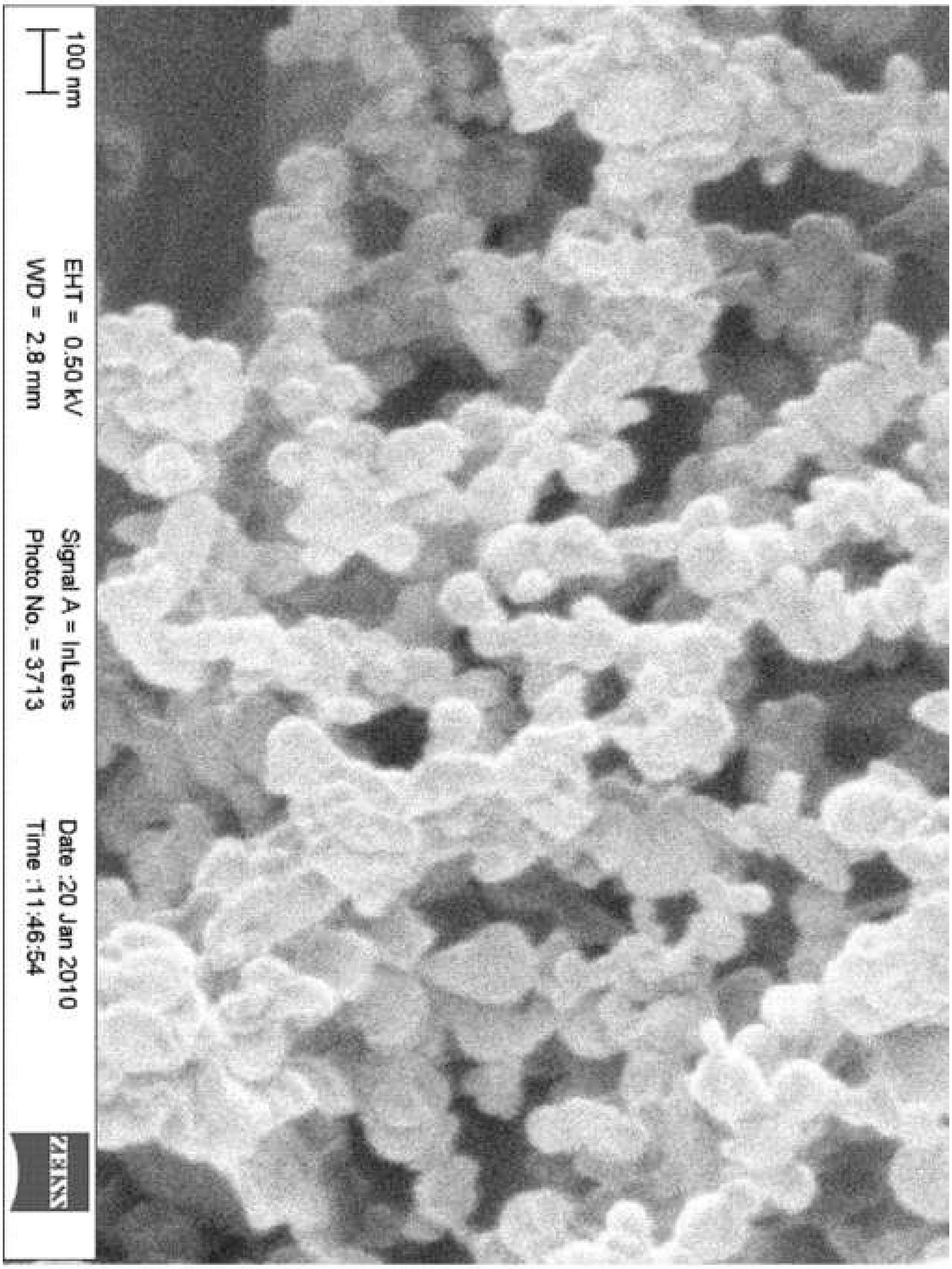

Figure E: Nano-CuO

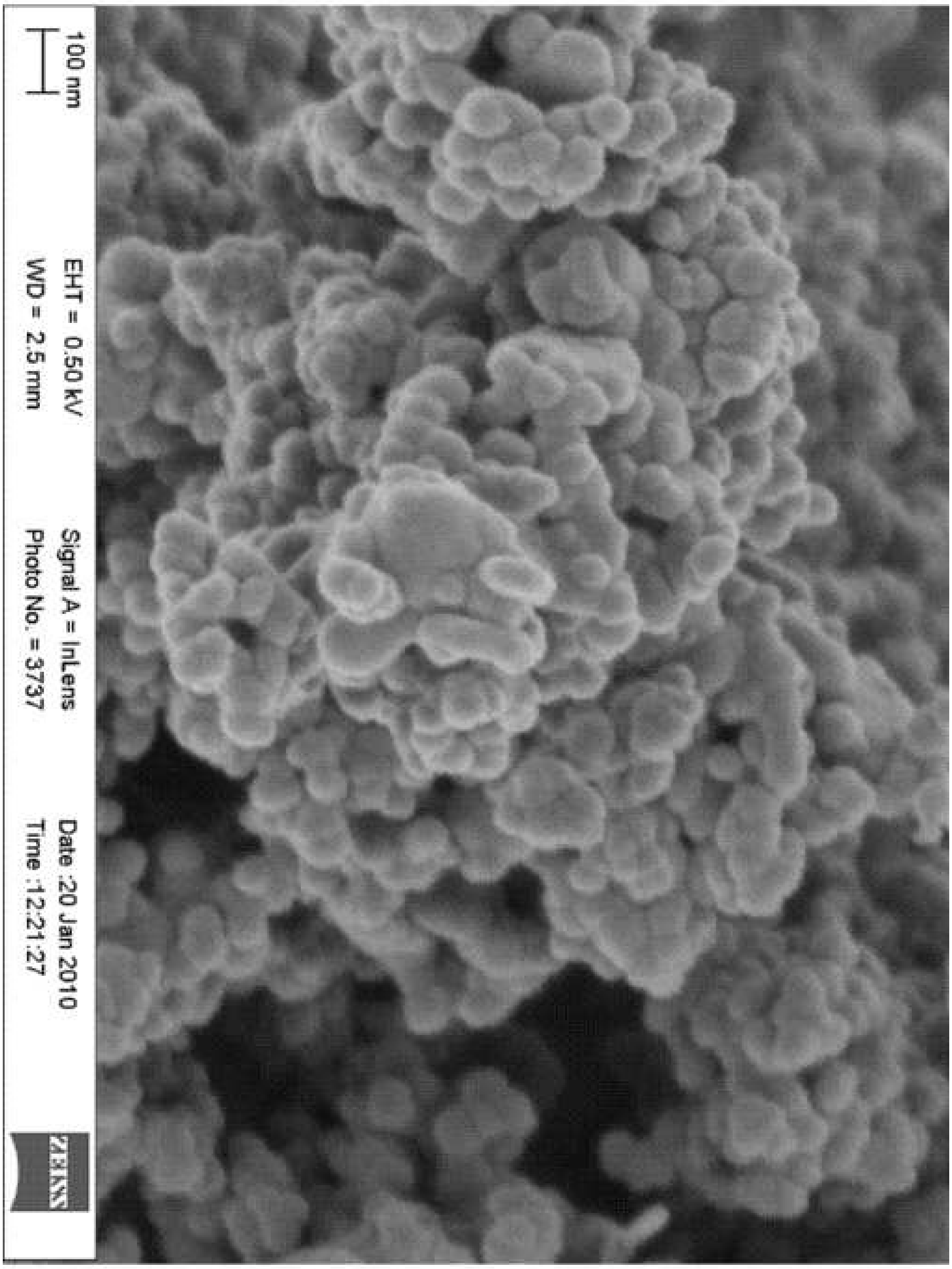

Figure F: Micron CuO

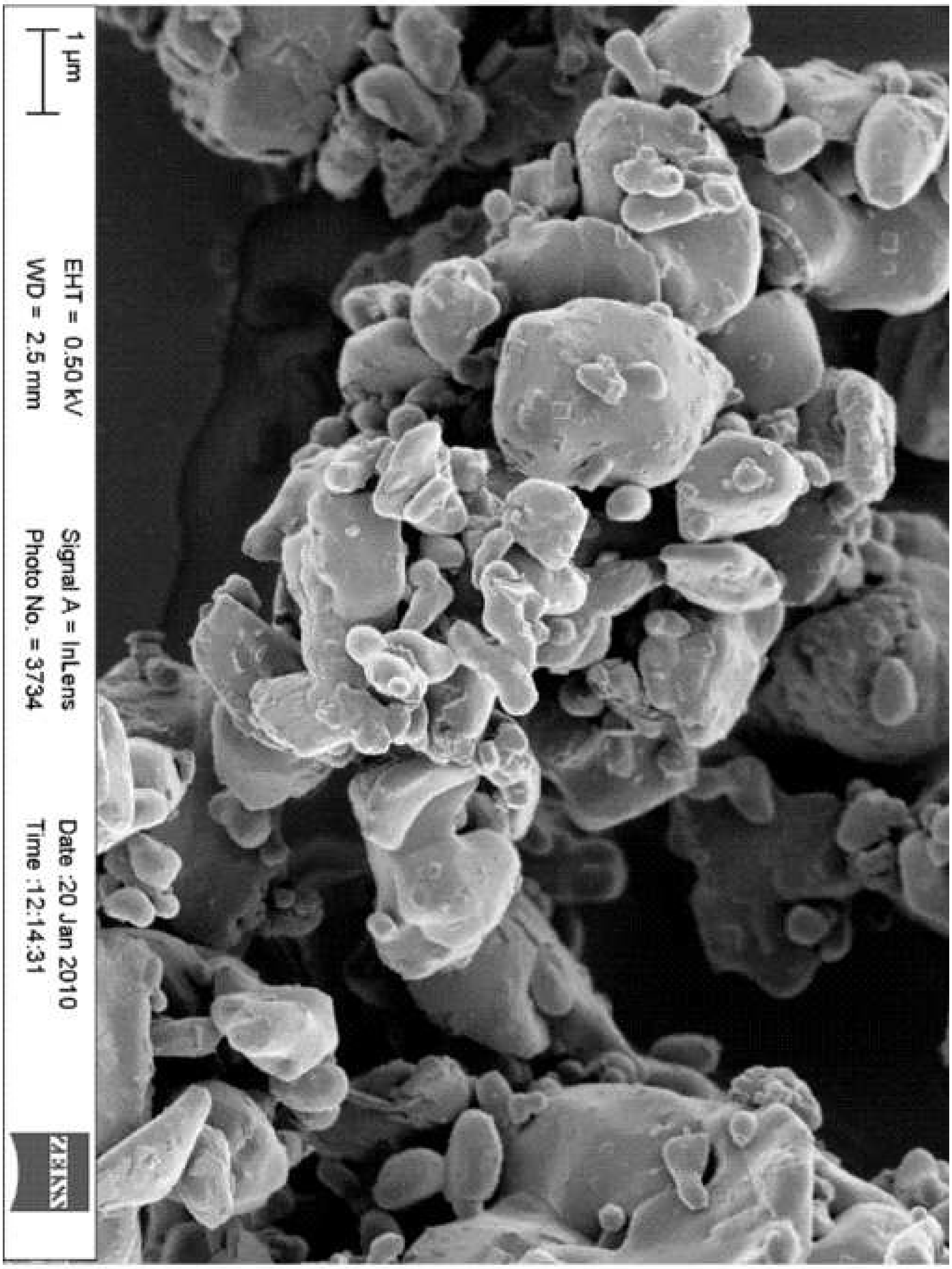

Figure G: Nano-Bi_2O_3

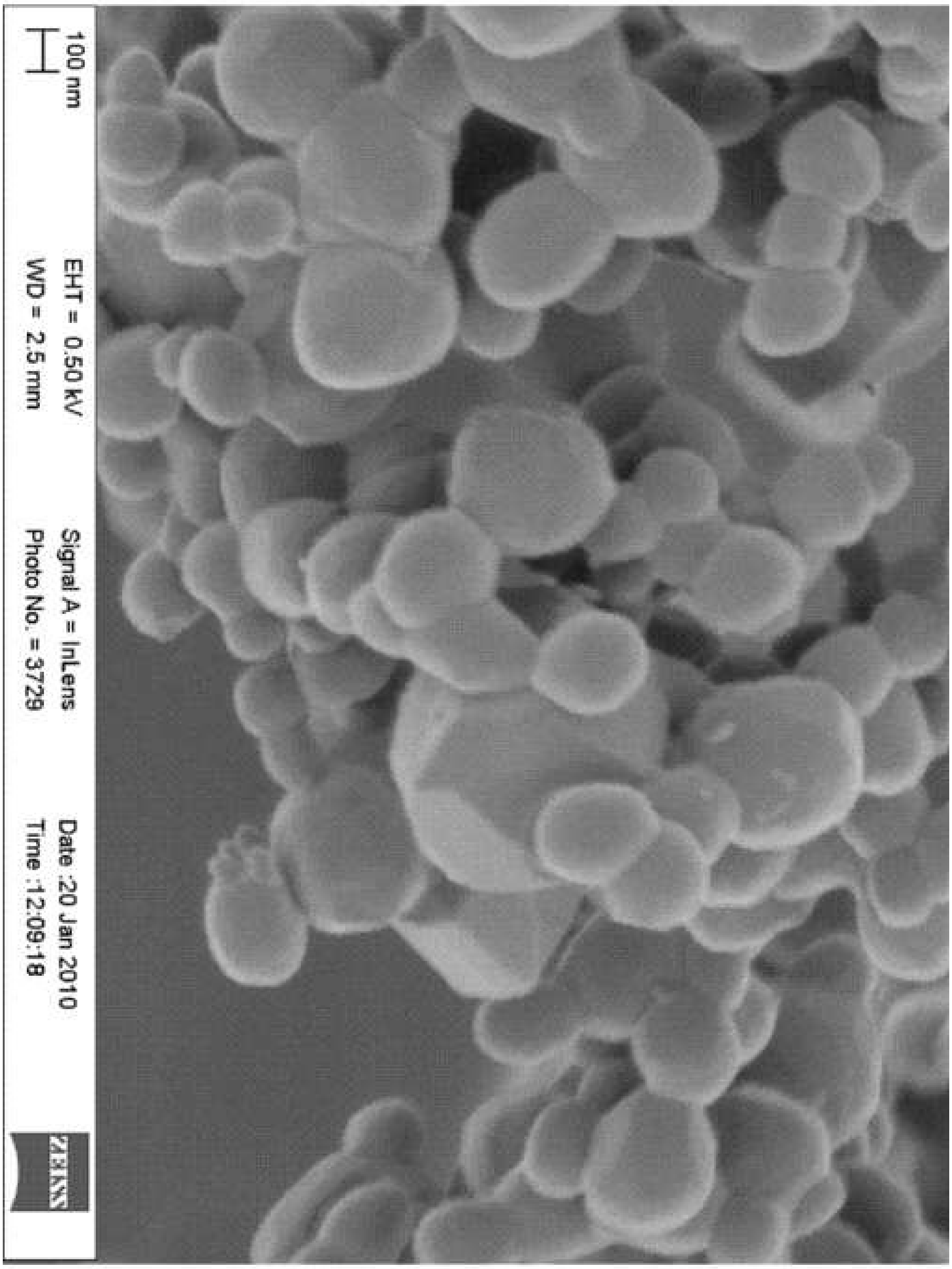

Figure F: Temperature vs. time for five identical trials of α-Al_2O_3

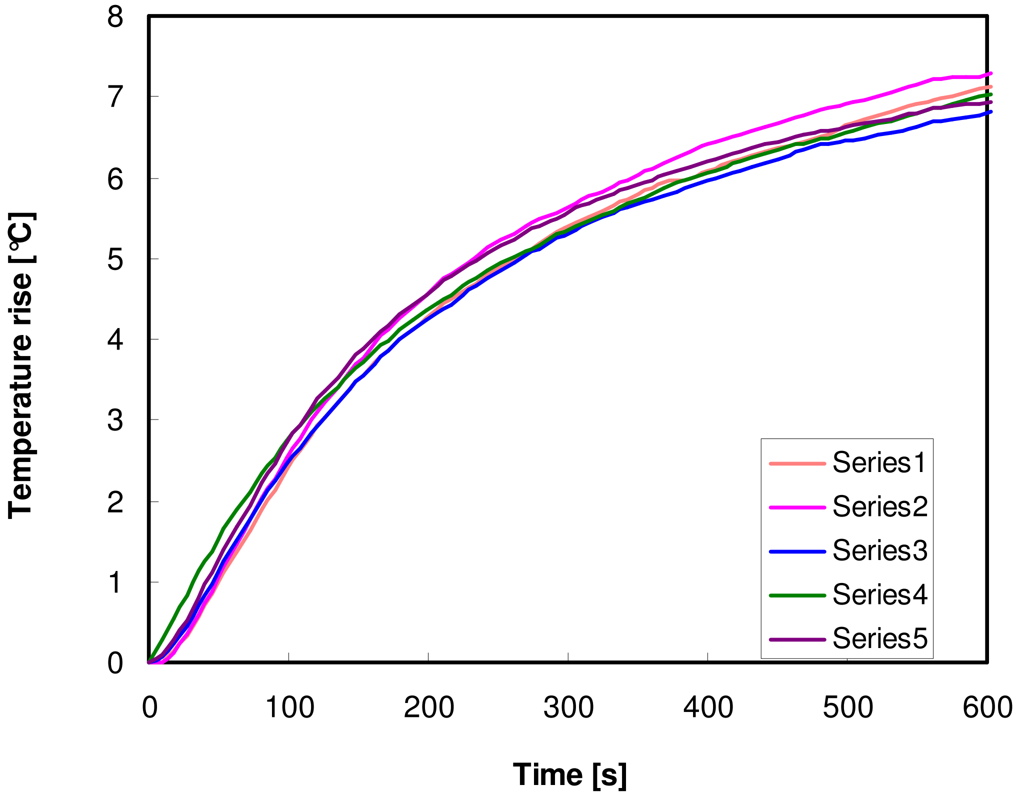

Figure G: Diagrams diagrams

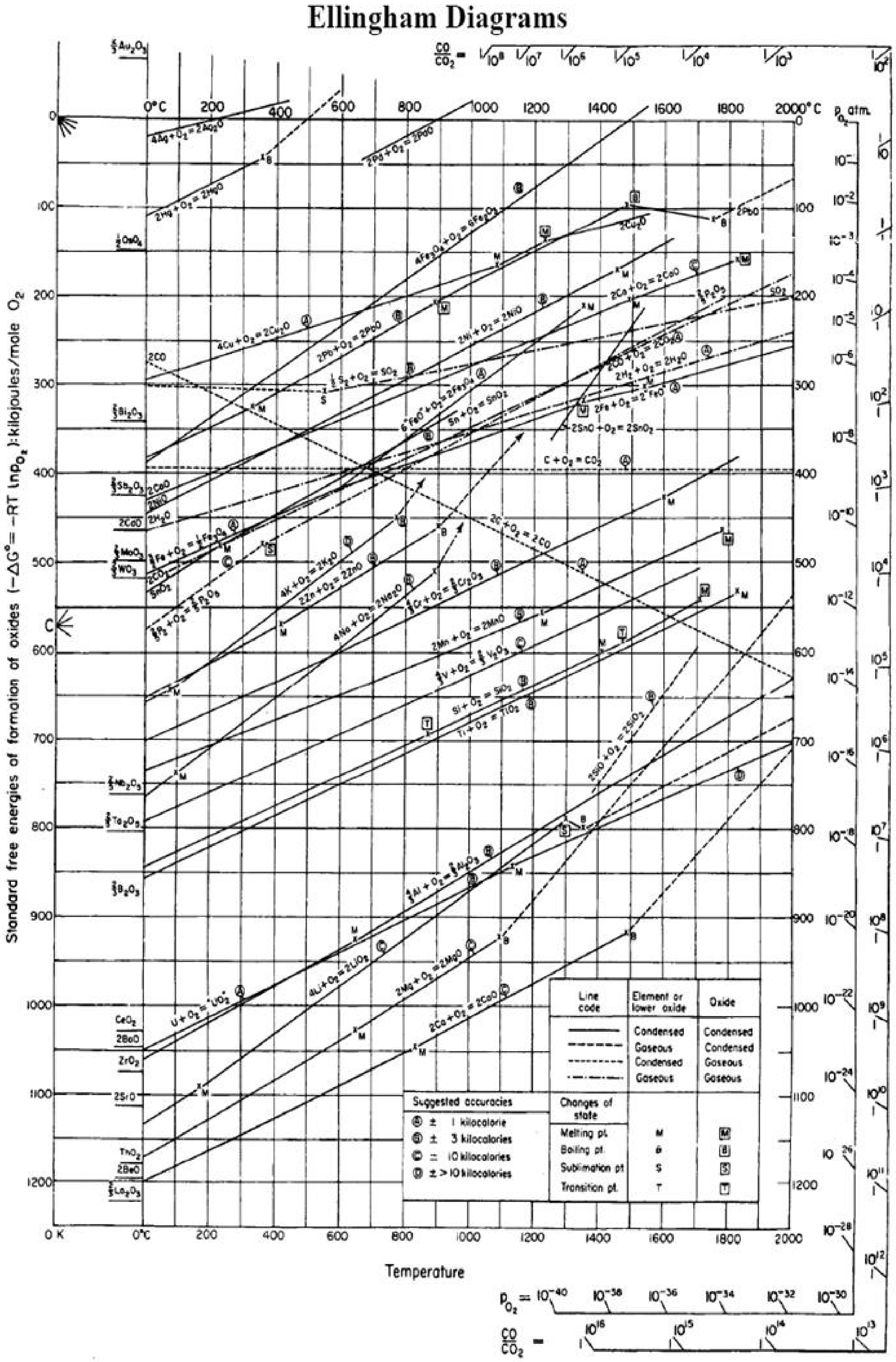

Carslaw and Jaeger equation

$$T= \frac{Q}{4\pi a\lambda}\left(1-\frac{2}{\pi}I\right)$$

with: $$I=\int_0^{\infty}\frac{e^{(-yu^2)}du}{[\left(\frac{u^2}{k}\right)-1]^2+u^2}$$

and:

$$y=\frac{\lambda t}{a^2\,\rho c}=\frac{Dt}{a^2}$$

Where:

D is the thermal diffusivity

u is the radial distance in the medium from the probe

a is the effective radius

Heat of reaction for Al/CuO thermite system

$2\,Al \quad + \quad 3\,CuO \quad \rightarrow \quad Al_2O_3 \quad + \quad 3Cu$

$2{*}26.98 \quad 3{*}79.54 \quad 101.96 \quad 3{*}79.54$

ΔH_f**:** -155.2 -1669.8

Stoichiometry: 19 81

Ratio of CuO/Al: 81/19

For 1 g of the mixture of CuO and Al, there is 0.81 g of CuO

Al_2O_3 formed: (101.96/3*79.54)*0.81

ΔH_r: 0.81*[-(101.96/3*79.54)*(1 669.8/101.96) + (155.2/3*79.54)]*1 000

The heats of reaction for different ratios were calculated in the same way and are listed in the table below.

Al (g)	CuO (g)	CuO in 1g	ΔH	(-)ΔH
15	85	0.64	-25 700.5	25 700.5
19	81	0.81	-32 527.2	32 527.2
25	75	0.75	-30 117.8	30 117.8
30	70	0.70	-28 110.0	28 110.0
35	65	0.65	-26 102.1	26 102.1
40	60	0.60	-24 094.3	24 094.3
45	55	0.55	-22 086.4	22 086.4
50	50	0.50	-20 078.5	20 078.5
60	40	0.40	-16 062.8	16 062.8